MODIFICATION OF UREA FORMALDEHYDE WITH NANOCELLUOSE DERIVED FROM A COMPOSITE OF BAOBAB POD FIBRE AND WASTE NOSE MASK (SYNTHETIC).

BY

IBRAHIM, Umar Farouq

MENG/SIPET/2018/8190

DEPARTMENT OF CHEMICAL ENGINEERING

FEDERAL UNIVERSITY OF TECHNOLOGY MINNA

OCTOBER, 2023

D ABSTRACT

This study focuses on the use of nanocellulose derived from baobab pod fibres and waste nose masks for modifying urea formaldehyde. The baobab pod fibres and waste nose mask fibres were characterized in terms of their properties, including chemical treatment to improve adhesive tendency with the reinforcement material. Acid hydrolysis was used to produce nanocellulose from the treated fibres, and the functional groups, surface morphology, and crystallinity of the fibres were investigated using Fourier Transform Infrared (FTIR), Scanning Electron Microscopy/Energy Dispersive X-ray Spectroscopy (SEM/EDS), and X-ray Diffraction. To modify the urea formaldehyde, compression moulding was used with a formulation of nanocellulose to urea formaldehyde ratios ranging from 10-90 wt%, 20-80 wt%, 30-70 wt%, and 40-60 wt%. The mechanical properties of the modified urea formaldehyde were then investigated. The results showed that the nanocellulose hydrolysed from baobab pod fibres and waste nose masks has excellent properties for modifying urea formaldehyde. The baobab pod fibres and waste nose mask fibres were found to be suitable for producing nanocellulose, as they exhibited favourable properties such as high cellulose content and low lignin and hemicellulose content. The acid hydrolysis process was effective in producing nanocellulose from these fibres, which exhibited high crystallinity and surface area. The SEM/EDS analysis also showed that the nanocellulose had a highly porous structure, which could potentially enhance its adhesion properties with the urea formaldehyde. The

modified urea formaldehyde produced using the nanocellulose showed improved mechanical properties, including increased tensile strength, modulus of elasticity, and elongation at break. The highest mechanical properties which are the tensile strength was observed in the samples with the highest nanocellulose content at 30%wt, indicating that the addition of nanocellulose had a positive impact on the properties of the urea formaldehyde. In conclusion, this study highlights the potential of using nanocellulose derived from baobab pod fibres and waste nose masks for modifying urea formaldehyde. The nanocellulose exhibited favourable properties, and its addition to the urea formaldehyde improved its mechanical properties. The findings of this study could have implications for the development of sustainable and eco-friendly materials in the future.

DI TABLE OF CONTENTS

DII LIST OF FIGURES

 LIST OF TABLES

Table Page

DIII LIST OF PLATES

CHAPTER ONE

1.0 INTRODUCTION

1.1 Background to the Study

Formaldehyde-containing adhesives account for approximately 95% of all wood adhesives used in the production of wood-containing composites and 85% of them are UF resins (Antov, et al, 2020). They owe their popularity to a number of advantageous properties, such as high reactivity, lack of colour, competitive price, and good performance in indoor environments. Their application may cause indoor air pollution and potential health issues because of the free formaldehyde emitted from the UFbonded wood-based panels. Substances such as formaldehyde, acetone, acetaldehyde, and ethyl-1-hexanol were found to be the main pollutants detected in indoor residential environments. These substances were also closely related to the occurrence of mucosal symptoms among the examined occupants. Many studies, performed both in vitro and in vivo, confirmed the toxic effects on various human or animal cells and organs such as the lung, upper respiratory tract, brain, and bone marrow in cases of formaldehyde occupational exposure. Taking into account the emerging reports on health hazards, the International Agency for Research on Cancer (IARC) re-classified formaldehyde from a “probable human carcinogen” to a “known human carcinogen” in 2004. One of the methods contributing to the reduction of formaldehyde emission from wood-based products is the introduction of proper additives, so-called formaldehyde scavengers, to the resins. These can be various types of substances such as chemicals, mineral particles, particles rich in phenolic substances, particles with high protein content, nanoparticles, etc. With the advances, in technology and the increase in the global population, plastic materials have found wide applications in every aspect of life and industries. However,

most conventional plastics such as polyethylene, polypropylene, polystyrene, poly (vinyl chloride) and poly (ethylene terephthalate), are non- biodegradable, and their increasing accumulation in the environment has been a threat to the planet (Tokiwa et al, 2009).

Due to the COVID-19 pandemic, wearing face masks to block the spread of the epidemic has become the simplest and most effective way. However, thousands of tons of medical waste of used disposable masks will be generated every day in the world, causing great pressure on the environment.

To overcome all these problems, some steps have been taken to reduce this waste. The first approach involves production of plastics with high degree of degradability. Synthetic plastics are resistant to degradation, and consequently their disposal is fuelling an international drive for the development of biodegradable polymers (Kolibaba et al., 2017)

These plastics remain in landfills and in the environment where they are unintentionally ingested by animals and are making their way up the food chain which proves to be a major ecological and environmental problem. Recently, there is a growing interest in replacing some or all of the synthetic polymers, like polyethylene, with biodegradable materials due to their environmental impacts (Islam et al, 2013).

There is a world-wide research effort to develop biodegradable polymers as a waste management option for polymers in the environment. Biodegradation (biotic degradation) is a chemical degradation of materials (polymers) processed by the action of microorganisms such as bacteria, fungi and algae. Biodegradation is considered a type of degradation involving biological activity. Biodegradation is expected to be the major mechanism of loss for most chemicals released into the environment. This process refers to the degradation and assimilation of polymers by living microorganisms

to produce degradation products. The most important organisms in biodegradation are fungi, bacteria and algae. Natural polymers (i.e., proteins, polysaccharides, nucleic acids) are degraded in biological systems by oxidation and hydrolysis. Biodegradable materials degrade into biomass, carbon dioxide and methane. In the case of synthetic polymers, microbial utilization of its carbon backbone as a carbon source is required (Leja, 2010).

The harmful effects on the ecology of long-lasting synthetic composites have led to increasing interest in the development of Eco composites based on more environmentally sustainable materials. Meanwhile, natural fibres reinforced polymer composites represent an opportunity to partially minimize on the environmental impacts by replacing biodegradable fibres such as flax, hemp, sisal, and wood particles with synthetic fibres such as glass, carbon or steel in composite materials production (Islam et al, 2013).

These materials must meet specific criteria set out by the ASTM and ISO in order to be classified as biodegradable. In general, the likelihood of microbial attack on a material is dependent on the structure of the polymer. When examining polymer materials from a scientific standpoint, there are certain ingredients that must be present in order for biodegradation to occur. Most importantly, the active microorganisms (fungi, bacteria, actinomycetes, etc.) must be present in the disposal site. The organism type determines the appropriate degradation temperature, which usually falls between 20 to 60^{o}C (Shetty et al, 2010). The disposal site must be in the presence of oxygen, moisture, and mineral nutrients, while the site pH must be neutral or slightly acidic (5 to 8) (Kolibaba et al., 2013)

1.2 Statement of the Research Problem

The limitations of urea formaldehyde (UF) resin, includes mechanical strength, water resistance, and environmental impact. The proposed solution is to modify UF with nanocellulose derived from baobab pod fibre and waste nose masks. However, there are knowledge gaps and challenges that need to be investigated thoroughly.

Baobab pod fibre was chosen as a source of nanocellulose due to several reasons. Firstly, baobab trees are widely distributed in various regions, and their pods are a readily available waste material. By utilizing baobab pod fibre, the research aims to promote sustainability and use the fibre of the baobab instead of it not been beneficial. Secondly, baobab pod fibre has shown promising properties as a source of nanocellulose, including its high cellulose content and potential for producing nanofibers with desirable characteristics. Exploring the potential of baobab pod fibre as a source of nanocellulose contributes to expanding the range of sustainable biomaterials available for composite modifications for other precursor available.

1.3 Justification of the Study

The study on the modification of urea formaldehyde with nanocellulose derived from baobab pod fibre and waste nose masks is justified due to its potential to reduce formaldehyde emissions, utilize waste materials, enhance performance, promote renewable and sustainable resources, and contribute to scientific innovation. The inclusion of waste nose masks offers opportunities for waste management, resource recovery, enhanced material performance, sustainability, and practical relevance, ultimately contributing to reducing waste pollution and developing sustainable materials with wide-ranging applications.

1.4 Aim and Objectives

The aim of this research is to modify urea formaldehyde with nanocellulose derived from baobab pod fibres and waste nose mask.

The objectives of this research work are as follows:

i. To prepare the materials through extraction of fibres from the pod, size reduction of the waste nose mask and their chemical treatment ii. To produce cellulose nanocrystals from the baobab pod fibre and nose mask through acid hydrolysis.

iii. To characterise the nanocellulose produced by using FTIR, SEM/EDX and TGA

iv. Modification and Characterization of Urea Formaldehyde

1.5 Scope of the Study

This research will focus on the isolation of cellulose nanocrystals form baobab pod fibres and used nose mask, characterization of the nanocellulose produced, modification of the urea formaldehyde and finally characterization of the modifiedurea Urea formaldehyde

CHAPTER TWO

2.0 LITERATURE REVIEW

2.1 Natural Fibres

All fibres which come from natural sources (plants and animals) and do not require fibre formation or reformation are defined as natural fibres (Niddles, 2001, Jacob et al., 2004). Natural fibres are used in the manufacture of composite because of their low cost, abundance, renewable, better formability and eco-friendly features. They have low mechanical strength; most natural composites have strong, stiff fibres in a matrix which is weaker and less stiff. These engineering composites are desired due to their low density, high corrosion resistance, ease of fabrication, and low cost (Ubi and Abdulrahman, 2015). Natural fibres derived from plants mainly consist of cellulose, hemicellulose, lignin, pectin and other waxy substances. Cellulose is the main chemical component of all plant-based natural fibres. It is the most noteworthy organic component produced by plants that is ample in the environment. Based on the source of origin of natural cellulosic fibres they are recognized by the chemical structure of cellulose in the bundle which provides strength and stability to the plant cell walls and the fibre. The low spiral angle of structural cellulose, its smaller fibre diameter, and together with longer fibre is preferable properties of natural fibre (Anteneh et al., 2021). Cellulose is composed of a long chain of glucose polymer units that are connected to form microfibrils (Faridulhassan et al., 2020).

In various applications, natural fibres extracted from plants are used as reinforcements in both thermoplastic and thermoset composites. Fig 1 shows the different structural constituents a plant fibre which consist of cellulose and other trace element, it can be

seen that, cellulose is highly crystalline polymer which contain as much as 80% of crystalline regions.

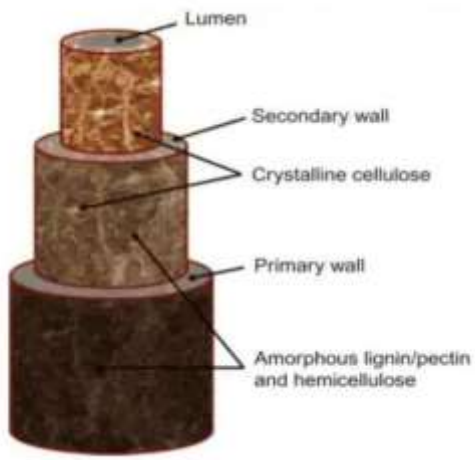

Figure 2.1: Structure of a plant fibre (Arun et al., 2020)

Hemicellulose is made up of highly branched polysaccharides attached to the cellulose after the removal of pectin. Lignin is amorphous, stiffens the cell walls, and act as a protective barrier for the cellulose (Zhu and Schmauder, 2003).

The reinforcing ability of natural fibres is usually enhanced by fibre treatment, which leads to improvement in the properties of fibre- reinforced resulting polymer composites (Idowu et al., 2016). Certain advantageous features, such as the biodegradability of natural fibres, coupled with the low cost, high specific strength and lighter weight than glass, have led to the extensive development of this environmentally friendly green material (Mohanty et al., 2000). Table 2.1 highlight some of the factors that differentiate between natural and synthetic fibres.

2.2 Classification of Natural Fibre

Fibres are a class of hair-like material that are continuous filaments or are in discrete elongated pieces, similar to pieces of thread. They can be spun into filaments, thread, or

rope. They can be used as a component of composites materials. They can also be matted into sheets to make products such as paper or felt. Fibres are of two types: natural fibres and manmade. Figure 2 shows classification of Natural fibres.

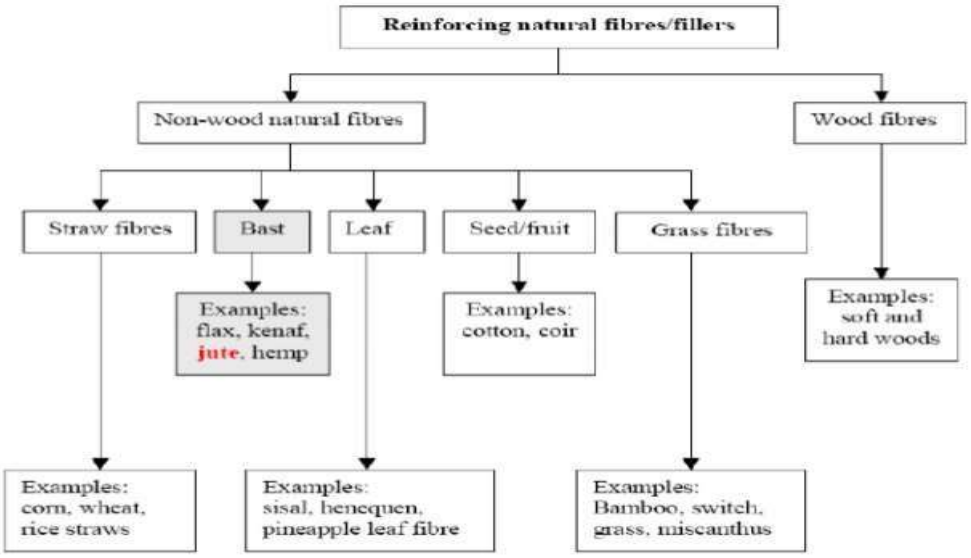

Figure 2.2: Classification of Natural Fibres (Mohanty et al., 2000)

2.2.1 Natural fibre reinforced composites

The interest in natural fibre-reinforced polymer composite materials is rapidly growing both in terms of their industrial applications and fundamental research. They are renewable, cheap, completely or partially recyclable, and biodegradable. Plants, such as flax, cotton, hemp, jute, sisal, kenaf, pineapple, ramie, bamboo, banana, etc., as well as wood, used from time immemorial as a source of lignocellulosic fibre, are more and more often applied as the reinforcement of composites. Their availability, renewability, low density, and price as well as satisfactory mechanical properties make them an attractive ecological alternative to glass, carbon and man-made fibres used for the manufacturing of composites. The natural fibre-containing composites are more environmentally friendly, and are used in transportation (automobiles, railway coaches,

aerospace), military applications, building and construction industries (ceiling panelling, partition boards), packaging, consumer products. (Zahra et al, 2017)

2.3 Baobab Tree

Adansonia digitata (L.) called the baobab tree in both English and French is very characteristic of the Sahelian region and belongs to the Malvaceae family (De Caluwé et al., 2010). The plant is a very massive tree with a very large trunk (up to 10 m diameter) which can grow up to 25 m in height and may live for hundreds of years. The plant is widespread throughout the hot and drier regions of tropical Africa (FAO, 1988).

Baobab tree as shown in Figure 3 has multi-purpose uses and every part of the plant is reported to be useful (Gebauer, 2010). The leaves, for instance, are used in the preparation of soup. Seeds are used as a thickening agent in soups, but they can be fermented and used as a flavouring agent, or roasted and eaten as snacks (Danfeu et al., 2016).

Figure 2.3: Image of a baobab tree (FAO, 1988)

The pulp is either sucked or made into a drink while the bark is used in making ropes (Igboeli et al., 1997). The different parts of the plant provide food, shelter, clothing and medicine as well as material for hunting and fishing (Venter & Venter, 1996). Baobab tree provides income and employment to rural and urban households.

2.3.1 Baobab pod fibres

Baobab (A. digitata L.), a tree plant belonging to the Malvaceae family, is widespread throughout the hot, drier regions of tropical Africa (FAO, 1988). It is a deciduous, massive and majestic tree up to 25 m high, which may live for hundreds of years, The trunk is swollen and stout, up to 10 m in diameter, usually tapering or cylindrical and abruptly bottle-shaped; often buttressed. Branches are distributed irregularly and large. The bark is smooth, reddish brown to grey, soft and fibrous (Gebauer, 2010). The trees consist of pods (fruits) as shown in Figure 4. The pod contains natural occurring fibres and a succulent material which contain vitamins.

Figure 2.4: Image of baobab pod fibres (Gebaur, 2010)

2.3.2 Baobab in polymer composite

The use of natural fibres as reinforcement in polymer composites is gaining attention recently, this is because of environmental issues, high cost and unsustainable nature associated with conventional synthetic fibres. Further, natural fibres have some advantages over their synthetic counterparts in term of physical, mechanical and biological properties; these include lower density, higher strength to weight ratio, higher specific properties, renewability and biodegradability. These make them useful in manufacture of bearings and linkages, building and automobile structures such as sliding panels c.

Fibres are the most important class of reinforcements, as they satisfy the desired conditions and transfer strength to the matrix constituent influencing and enhancing their properties as desired. Fibres fall short of ideal performance due to several factors. The performance of a fibre composite is judged by its length, shape, orientation, composition and the mechanical properties of the matrix (Nissen and Stutz 1985).

Microorganisms mostly consume the fibre parts. Composites reinforced with larger fibre length showed higher degradation rate. Higher fibre loading gives microorganisms larger surfaces to consume and results higher degradation rate. Over time larger surfaces became smaller and became easier target for microorganisms. (Winnie, 2021)

2.4 Waste Nose Mask

Influenced by recent COVID19, wearing face masks to block the spread of the epidemic has become the simplest and most effective way. However, after the people wear masks, there are also some inevitable but not enough attentions to follow-up problems, among which the most important is how to deal with the used disposable masks. If the average weight of a common three-layer disposable mask is 5g, thousands of tons of medical

waste will be generated every day in the world, causing great pressure on the environment. The structure of the common disposable mask is divided into three parts: the mask body, the ear straps and nose seals. The mask body is a non-woven fabric composed of high fluidity polypropylene (PP) resin, the ear straps were elastomer composed of polyurethane, and the nose seals were composed of iron wire and polypropylene resin. In addition to the fact that the nose seals are difficult to be reused because of the iron wire, polymer composites with high performance and high added value could be easily prepared by using the structural characteristics of the rest parts of the disposable mask, which has good ecological and economic benefits, and is helpful to solve the problems of environmental pollution and resource shortage in our society.

Another problem after the covid-19 pandemic is waiting at the door, disposal of used mask. As if now government advised people to use double mask, it means every individual will at least use a single surgical mask. Usually after the use of masks they are dumped in the household waste. Which are then taken to landfills and get mixed with other wastes This can be harmful to cleaners, marine life and many more. The best possible way to get out of this problem is to RECYCLE the used masks. Research shows that the improper disposal of used surgical masks is leading to waste generation and polluting the water bodies. The surgical masks are made of non-woven polypropylene (PP), PP can be recycled by converting into granules and then reinforcing it with hybrid fibre reinforcement.

2.5 Composite Materials

When a material is reinforced, it is most likely to form a composite. According to the dictionary of composite material technology, composite is a multiphase material formed from a combination of materials which differ in composition or form, remain bonded

together and retain their identities and properties. Composites maintain an interface between components and act in concert to provide improved specific or synergistic characteristics not obtainable

by any of the original components acting alone. Modern composite materials constitute a significant proportion of the engineering materials market ranging from everyday products to sophisticated niche applications. While composites have already proven their worth as weight-saving materials, the current challenge is to make them cost effective. The efforts to produce economically attractive composite components have resulted in several innovative manufacturing techniques currently being used in the composite industries. It is obvious, especially for composites, that the improvement in manufacturing technology alone is not enough to overcome the cost hurdle. It is essential that there be an integrated effort in designing, material processing, tooling, quality assurance, manufacturing, and even programme management for composites to become competitive with metals (Mohanty et al., 2000).

The composites industry has begun to recognize that the commercial applications of composites promise to offer much larger business opportunities than the aerospace sector due to the sheer size of the transportation industry. Thus, the shift of composite applications from aircraft to other commercial uses has become prominent in recent years (Dipen et al, 2019). Increasingly enabled by the introduction of newer polymer resin matrix materials and high-performance reinforcement fibres of glass, carbon and aramid, the penetration of these advanced materials has witnessed a steady expansion in uses and volume. The increased volume has resulted in an expected reduction in costs. High performance FRP can now be found in such diverse applications as composite armouring designed to resist explosive impacts, fuel cylinders for natural gas vehicles,

windmill blades, industrial drive shafts, support beams of highway bridges and even paper making rollers. For certain applications, the use of composites rather than metals has in fact resulted in savings of both cost and weight. Some examples are cascades for engines, curved fairing and fillets, replacements for welded metallic parts, cylinders, tubes, ducts, blade containment bands etc. (Chattopadhyay, 2004).

2.5.1 Composite manufacturing technique

Manufacturing of FRP composite involves manufacturing of fibre and then reinforcing these fibres with the matrix material by various techniques. Fibre preforms involve weaving, knitting, braiding, and stitching of fibre in long sheets or mat structure.

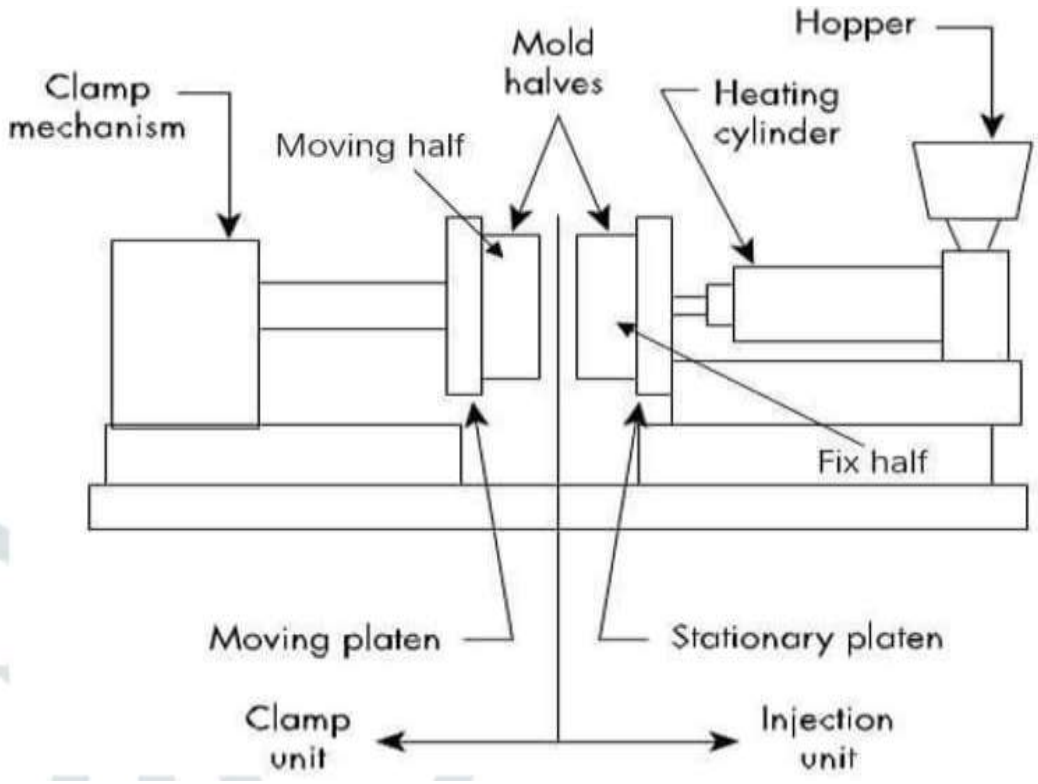

Figure 2.5: Moulding Machine Diagram (Mohammed et al, 2015)

Preforms are used to achieve a high level of automation with the assistance of robotics, which offers control over the fibre angle and the fibre content on every zone of the part to be moulded. It uses preheated moulds mounted on a hydraulic or mechanical press. A prepared reinforcement package from prepreg is placed in between the two halves of the mould, which are then pressed against each other to get a desired shape of the mould. Figure 3 represents the stepwise processing of compression melding. (Mohammed et al, 2015)

2.6 Cellulose Nanocrystals

Cellulose nanocrystals could have diameters up to 20 nm and lengths up to a few hundred nanometers. Potential applications of cellulose nanocrystals, including reinforcement of nanocomposite (Nguyen et al., 2020). Cellulose is a linear chain of anhydro glucose monomer units connected through 1–4 b-linkages, having amorphous and crystalline regions. Different sources of cellulose will yield distinct structures, properties and sizes of cellulose. Cellulose nanocrystals production could be varied depending on the sources from which it is extracted, which provides researchers with a broad range of choices to study, such as types of cellulose sources, reaction parameters and processing methods.

Plants are the primary potential sources of cellulose as plants are relatively cheap and abundant. Intrinsic structural variation in sources of the lignocellulosic materials and the isolation methods used can affect the size, morphology, and crystallinity of the cellulose nanocrystals extracted. (Hazrol et al, 2019)

2.6.1 Cellulose nanocrystals production methods

Cellulose nanocrystals isolation from lignocellulosic arrays of empty fruit bunches necessitates a series of processes. This series of processes can generally be divided into two stages: the first stage is the pretreatment and the second stage is the cellulose nanocrystals isolation (Choong et al., 2018). Chemical pretreatment is to eliminate extractives, lignin and hemicellulose content from the empty fruit bunch fibres. Various types of extractives exist in empty fruit bunch fibres, such as lignans, flavonoids, waxes and complex phenolics (Yakubu et al., 2017). However, after the chemical pretreatment step, pretreatment is only half-completed. The bleaching process using chlorine dioxide, sodium percarbonate, or hydrogen peroxide is necessary to obtain the desired degree of whiteness and remove the remaining extractives. The bleaching process using sodium hypochlorite is usually not encouraged due to the formation of dioxins, a toxic organic compound (Yakubu et al., 2017).

Subsequently, cellulose nanocrystals can be extracted by hydrolysis under controlled conditions. The most commonly used hydrolysis agent is mineral acid. As the amorphous region subsides in the remaining cellulose is relatively weak, it is susceptible to acid attack and destruction, leaving only cellulose with substantial crystalline segments (El Achaby et al., 2018). At the acid hydrolysis stage, cellulose nanocrystals extracted are needle-shaped nanoparticles with high surface area, aspect ratio and crystallinity (Yakubu et al., 2017). Homogenization will typically be required in the next step to uniformly disperse the cellulose nanocrystals that are contained in the suspension as tiny particles (which are having a high tendency to agglomerate). Finally, the cellulose nanocrystals suspension will be freeze-dried to obtain a bright-white solid sample.

2.6.2 Cellulose nanocrystal extraction after pretreatment

Isolation of cellulose nanocrystals is the second stage in the production of cellulose nanocrystals from the fibre source. Isolation of cellulose nanocrystals usually involves acid hydrolysis at elevated temperatures, which is targeted to reduce polymerization by breaking down the accessible amorphous regions of the long glucose chains, liberating the crystalline materials from the fibre source. Other methods, including enzymatic hydrolysis and ionic liquid, can be used to iso- late cellulose nanocrystals. Subsequently, the post-treatment of hydrolyzed celluloses, including sonication and purification, can be used to ensure the cellulose nanocrystals extracted are well-dispersed (Chieng et al., 2017).

In some of the research works, the effectiveness of chemical treatment could be enhanced by the presence of mechanical treatment during the isolation of cellulose nanocrystals from empty fruit bunches. For instance, cellulose nanocrystals with diameters from 5 to 40 nm and crystallinity values of 69 to 70% were successfully obtained from Elaeis guineensis empty fruit bunches through chemo-mechanical treatment (Harshai et al., 2019). However, mechanical or sonication treatment will not be considered one of the isolation methods in this study. Their roles are to assist the penetration of chemicals into the cellulose structures, which could further enhance the reactivity, thus the yield of cellulose nanocrystals.

2.6.2.1 Sulphuric acid hydrolysis

Cellulose nanocrystals are commonly prepared by acid hydrolysis of a purified cellulose starting material such as cellulose micro-fibres (CMF). The acid is used to hydrolyze the amorphous region of the cellulose, in which the disordered regions of cellulose can be disintegrated by hydrolytic cleavage of the glycosidic bond. In contrast, the highly ordered cellulose fractions will remain unconverted as they are less

susceptible to acid attacks (Chieng et al., 2017). Acid hydrolysis can produce a suspension of rod-like whiskers whose dimensions rely on cellulose origin and the pretreatment. Typically, the length and diameter of cellulose nanocrystals are less than 1 mm and 100 nm, respectively, with- out agglomeration (Chieng et al., 2017).

The hydrolysis of cellulose by sulphuric acid also involves partial esterification of the hydroxyl groups, as shown in 4. Esterification causes the attachment of negatively charged sulphate groups to the cellulose nanocrystals structure. Esterification induces the repulsion forces between cellulose layers that can prevent cellulose nanocrystals from forming aggregates. The attachment of negatively charged sulphate groups on the cellulose nanocrystals structure phenomenon is also known as anionic stabilization (Chieng et al., 2017).

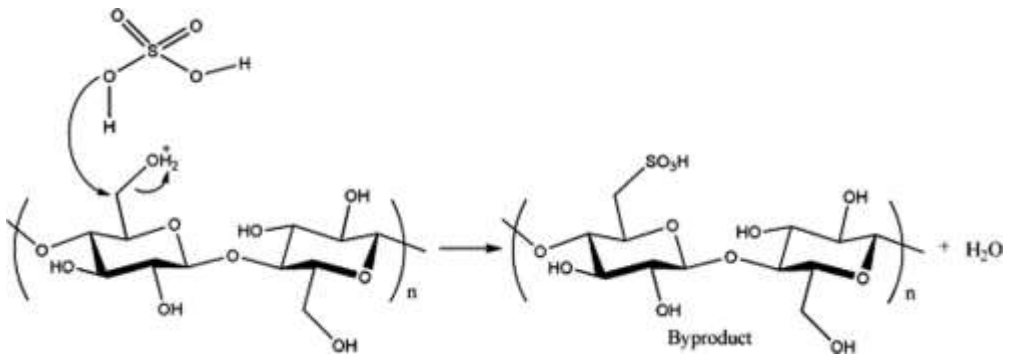

Figure 2.6: Mechanism of cellulose nanocrystals esterification (Peet et al., 2017)

2.6.2.2 Hydrochloric acid hydrolysis

One of the initiatives to evaluate the effectiveness of hydrochloric acid in hydrolyzing the empty fruit bunches was conducted by a group of researchers from Japan (Hastuti et al., 2018). In their study, the bleached empty fruit bunches, alkaline-treated bleached empty fruit bunches, and alkaline- treated bleached empty fruit bunches soaked in hot water at 60 °C, were suspended in 100 ml 3 M

HCl at 80 °C and continuously stirred for 2 h.

2.6.2.3 Phosphotungstic acid hydrolysis

Another group of researchers also have introduced the application of solid acid in hydrolyzing the empty fruit bunch fibres for cellulose nanocrystals isolation (Budhi et al., 2018), which could have several advantages in comparison to the liquid phase mineral acids such as ease of acid recovery, good thermal stability, and safe working environment. Researchers have introduced Phosphotungstic acid (a kind of solid acid) from 65 to 85% in treating one gram of pulp in an Erlenmeyer at a temperature range of 80 to 100 °C under a continuous mechanical stirring for duration of 25 to 35 h. The resulting solution (after the reaction process was stopped using a chilled water bath) was extracted using diethyl ether in excess to form a solution with 3 layers. The lowest layer of the solution consisted of Phosphotungstic acid and diethyl ether, while the middle layer consisted of cellulose nanocrystals, water, and degraded sugar. The upper layer of the solution, however, consisted of mainly diethyl ether.

2.6.3 post-treatment of cellulose nanocrystals

Cellulose nanocrystals extracted from empty fruit bunch fibres may require modification depending on the applications of the cellulose nanocrystals. The posttreatment of the cellulose nanocrystals will typically involve the surface modification of the samples using various additives that can alter the surface properties of the cellulose nanocrystals. Cellulose nanocrystals can be functionalized by altering the surface hydroxyl groups, which can enhance their properties such as conductivity, hydrophobicity (Mohammed et al., 2021), and thermal responsiveness (Miyashiro et al,

2020). This section will discuss some of the reported works that employed post-treatment on cellulose nanocrystals.

2.7 Urea Formaldehyde Resin

Urea-formaldehyde (UF) products (also called aminoplasts) are highly crosslinked, semi-crystalline thermosetting plastics; which is the product of a condensation reaction between urea and formaldehyde (Park and Jeong, 2011). The UF resins are noted for their high strength, rigidity, cost effectiveness, and fast cure. UF resins are among the fastest curing resins available. At elevated temperatures, they can be cured in as little as two, A large portion of UF resins is consumed by the wood products industry; most especially, it serves as adhesives for particleboards (Dunky et al., 2012). The popularity of urea-formaldehyde resins as the main adhesive for wood products has several reasons, including low cost, ease of use under a variety of curing conditions, versatility, low cure temperature, resistance to mold formation, excellent thermal properties, lack of color of the cured product, and excellent water solubility of the (uncured) resin. A major drawback of urea- formaldehyde adhesives compared with other thermosetting wood adhesives, such as phenol-formaldehyde and polymeric diisocyanatos, is the lack of moisture resistance especially at elevated temperatures. Furthermore, the reversal bondforming reactions can lead to the release of formaldehyde. (Tomita & Hatono, 1978)

Urea formaldehyde (UF) resins are primarily made up of urea and formaldehyde with formaldehyde acting as the cross linker. The UF resins are formed in water at a pH above 7 at the start of the reaction, because the methylol derivatives that form in the first steps condense rapidly at acidic conditions, as illustrated in scheme (1):

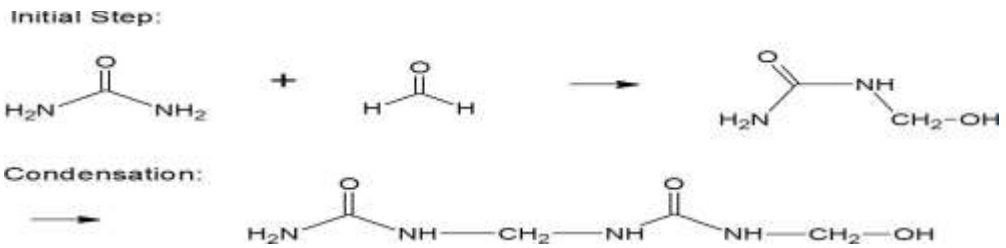

Figure 2.7: Reaction Urea with formaldehyde and condensation reaction of the methylol group formed

Under alkaline conditions, on the other hand, in scheme (2), the condensation is much slower and better to control. Instead of methylene linkages, di-ethylene ether groups form:

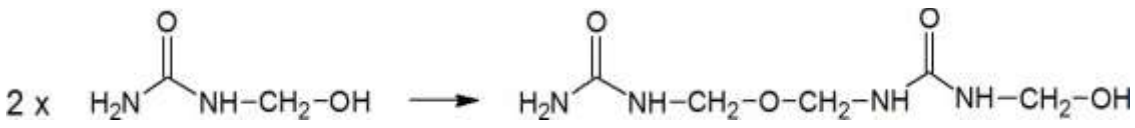

Figure 8: Formation of di-ethylene ether groups.

The condensed oligomers are water soluble and contain hemi formal groups. This mixture is further reacted under acidic conditions (usually at about pH 5) and by heating, which leads to the desired degree of condensation.

In the case of surface coatings, the UF resins are often modified to improve their solubility in solvent, for example, by reacting them with n-butyl alcohol (etherification) prior to condensation (resin formation).

Taking into account the emerging reports on health hazards, the International Agency for Research on Cancer (IARC) re-classified formaldehyde from a “probable human carcinogen” to a “known human carcinogen” in 2004 (Kristak, et al., 2022). Its emission from UF resins is mostly sourced from the unreacted formaldehyde, hydrolytic

degradation of bond lines under moisture conditions, and the reversibility of amino methylene link in the cured adhesive network (Park and Jeong, 2011). One of the methods contributing to the reduction of formaldehyde emission from wood-based products is the introduction of proper additives, so-called formaldehyde scavengers, to the resins. These can be various types of substances such as chemicals, mineral particles, particles rich in phenolic substances, particles with high protein content, nanocrystals from baobab pod fiber etc.

2.8 Application of Natural Fibre Reinforced Polymer Matrix Composites The applications of natural fibre reinforced polymer matrix composites are growing rapidly in many engineering fields. These composites find use in various industrial and structural applications, such as aircraft, automotive, sporting goods, marine, infrastructure, electronics, furniture and building construction industries

Natural fibre reinforced polymer matrix composites are used in the production various parts of an automobile. The manufacturing process for making parts to be used in industrial applications requires good finishes, which can be achieved with compression moulding. Examples of compression moulded automotive parts using natural fibre reinforced polymer matrix composites include, bumper covers, roof frames, door frames, door panels, engine valve covers, dash boards and truck car mats.

The use of NFs as a potential substitute to synthetic fibres in reinforcing polymer matrices has increased in recent years due to environmental concerns. Among the reviews on NFs, there were missing comprehensive study on the chemical composition, spatial distribution and concentration of the chemical compositions, water absorption behaviour and thermal properties of baobab pod fibre. Also, there are no comprehensive studies on the effect of chemical treatments and varying fibre contents on the physical,

mechanical and thermal properties of baobab fibre reinforced UF composites using extrusion and compression moulding techniques. These missing research gaps gave the motivation to fully study the properties of baobab fibres and its use in UF modification.

CHAPTER THREE

3.0 MATERIALS AND METHODS

The materials, equipment and experimental procedures used during the course of this research are presented in this chapter.

3.1 Materials

The starting materials for this research work are baobab and waste nose mask as shown in Figure 9 (a) and (b) respectively

Plate I: Images of (a) waste nose mask and (b) Baobab pod fibres

Table 3.1: Materials used for the research work

Material	Purity	Source
Urea, formalin	37%	Chemical vendor
Distilled water	100%	Chemical vendor
Baobab pod fibre	Standard	Central market Kaduna
Sodium hydroxide (NaOH) pellets	98%	Chemical vendor
Waste nose mask	Standard	Streets of Abuja
Hydrochloric Acid	Standard	Chemical vendor

3.2 Methodology

The steps involved in these experimental processes for the modification of urea formaldehyde with nanocellulose derived from baobab pod fibres and waste nose mask materials are summarised in the process flow diagram shown in Figure 10.

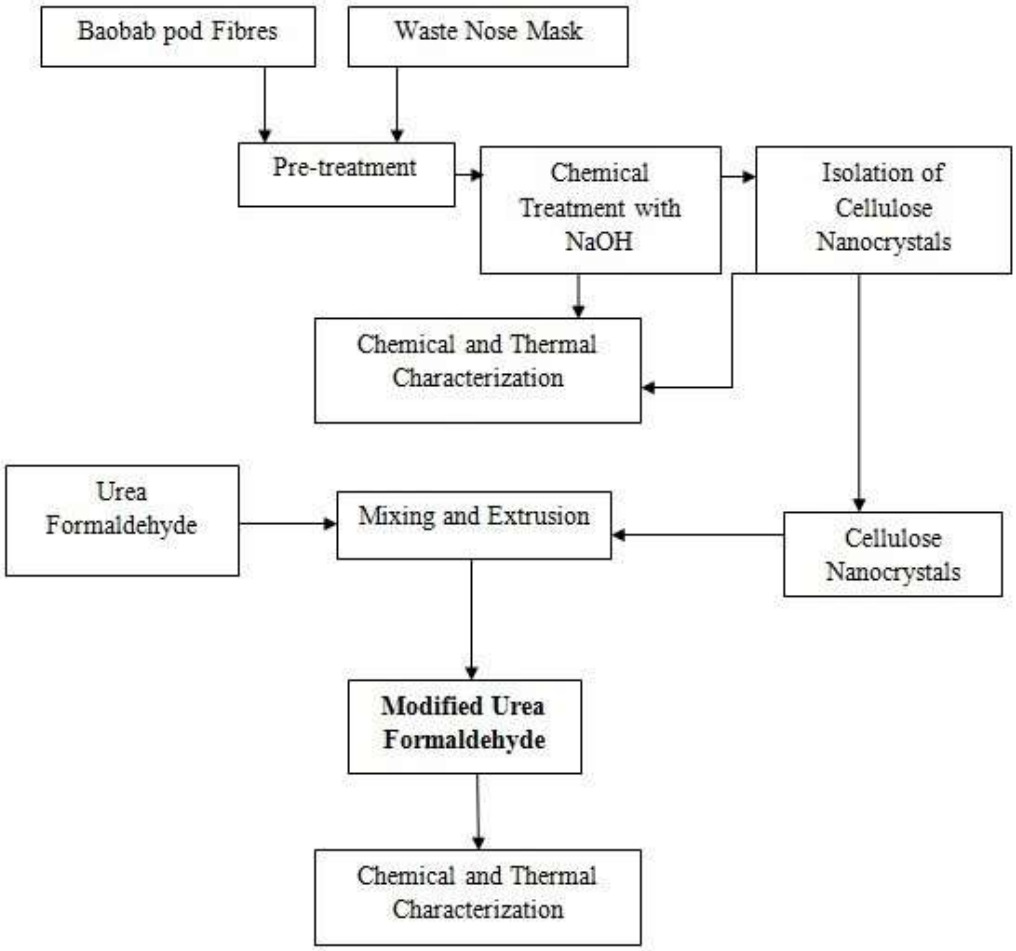

Figure3.1: Experimental Process Diagram for UF Modification

3.2.1 Extraction of Baobab fibres

Ripe and mature baobab pods about 0.635 cm thick, 20 cm high and 10 cm in radius, were flocked from baobab tree. They were sliced open mechanically using a metal cutter. Each mature pod holds about 30 g of baobab fibre in combined state with fruit pulp. The fibres were screened out from the sweet condolence by hand, and then been

washed in a running tap water to remove the remaining pulp that gummed the fibres together. Finally, the fibres were dried for 24 h; the fibres were then ground and sieved as shown in Figure 11.

Plate II: Ground Baobab pod fibres

3.2.2 Treatment of Baobab fibre and waste nose mask

Sodium hydroxide solutions were prepared in 1000 ml beaker each by diluting 40 g pellets of sodium hydroxide in 800 ml of distilled water to give a 5 wt% of NaOH solution. Baobab pod fibres and Waste Nose Mask were soaked in the prepared 5 wt% of NaOH solution separately and heated at 40^{o}C for 1200s (20min) on a regulated hot plate under a continuous stirring to ensure even modification. The distilled water was used to rinse the fibres until a neutral pH and then dried. The treated fibre is shown in Plate III.

Plate III: Chemically treated Baobab pod fibres and Waste Nose Mask

3.2.3 Preparation of waste nose mask

The used nosed masked were collected from various sources, it was then dusted and cleaned. After cleaning, they were washed in running tap water and allowed to dry for 24 h. The masks were then toned into small pieces using bear hands. After the preliminary size reduction, a ball mill was used to further reduce the size into very tiny pieces and then sieved. Very fine particles were obtained and stored separately.

500 grams of the powdered materials obtained from the waste nose mask and 500 grams of that received from the baobab pod fibres were then combined together and taken for acid hydrolysis.

3.3 Preparation of Nanocellulose by HCl Acid Hydrolysis

Three stages were involved in the isolation of cellulose nanocrystals from Baobab pod fibres and waste nose mask material, these includes sodium hydroxide treatment, bleaching with sodium chlorite and acid hydrolysis using hydrochloric acid.

3.3.1 Bleaching with sodium chlorite ($NaClO_2$)

Hydrochloric acid (HCl) method was used for the bleaching of Baobab pod fibre and the waste nose mask. 1.5 w/v% HCl was prepared in a 500 cm^3 beaker and Baobab pod fibres and waste nose mask was immersed into the solution and heated for 5 h at 90 ℃. The resulting solution was then washed with water; the fibres were then dried in an oven for 2 h at 50 ℃. Bleaching removes the surface colour of the material as can be seen in Plate IV.

Plate IV: Bleached Baobab Fibres and Waste Nose Mask

3.3.2 Acid hydrolysis

Analytical grade NaOH was used. Different concentrations of aqueous NaOH were prepared by dissolving NaOH pellets in distilled water. Ground BPFs were then immersed into the solution and heated for 4 h with a solution to fibre ratio of 40 cm^3 to 1 g. A formulation of 60 % Hydrochloric acid (HCl) was used for the isolation of cellulose. 10 g of bleached BPFs and 10 grams of ground waste nose mask were placed in a conical flask. 160 cm^3 of acetic acid were added and the flask was then closed using

a cork. It was then placed on a heating mantel at a temperature of 90 °C for 40 min. The flask was then removed from the heating mantel and cooled before 70 cm^3 distilled water was added. The digested solution for the baobab and waste nose mask are shown in Figure 14

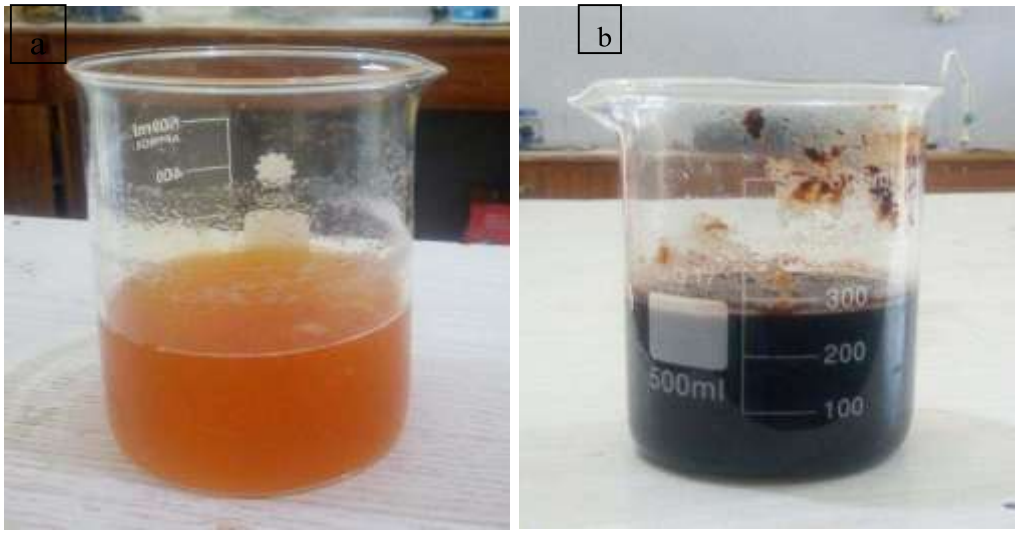

Plate V: (a) Digested Baobab Fibres and (b) Digested Waste Nose Mask

3.3.3 Centrifugation

A centrifuge was used to wash the hydrolysed cellulose several times; the centrifugation took place at 1000 rpm, 20 min and 10 ℃. the products were then neutralized to a pH of

7.

3.4 Characterization of Cellulose Nanocrystals

Various characterization techniques and instrumentations are introduced to investigate the surface morphology, topography, crystallographic structure, elemental and thermal properties of cellulose nanocrystals extracted from empty from baobab pod fibers and waste nose mask. Different characterization techniques reveal different information about the analyzed sample. As for crystallographic structures, elemental properties,

and thermal stabilities, cellulose nanocrystals can be analyzed using an X-ray diffractometer (XRD), Fourier transform infrared spectroscopy (FTIR), and thermogravimetry, respectively.

3.5 Synthesis of Urea Formaldehyde

In this study, synthesis of UF resins was carried out following the conventional alkaline-acid two-step reaction. The pH of addition and condensation reaction was 7.8 and 4.6, respectively, with an addition of second urea, resulting in F/U mole ratio around 1.0, namely 0.95; 1.05, and 1.15. For higher mole, UF resin with F/U mole of 2.0 was also prepared.

The reaction is influenced by several parameters. It requires precise control of purity, amount and sequence of addition of the raw materials, alkaline and acid catalysts. The preparation conditions are adjusted and monitored with respect to temperatures, pH, and concentration of the reactants. Initially, the resin was reacted with an alkaline catalyst to initiate the addition reaction, and at the appropriate reaction time the resin solution was converted to the acid side to promote the condensation reaction.

Synthesis of UF resins in the laboratory was carried out based on conventional two step reactions, consisted of methylolation or addition reaction and condensation reaction. Briefly, the formalin is placed in the glass cooking reactor with the mantle heater and the condition is adjusted into pH 7.8~8.0. Then, the 1st urea is placed into the reactor, yielding a molar ratio F/U of 2.0. The mixture is heated to 90°C for one hour to allow the methylolation reaction. The temperature is then adjusted to 80°C and the condensation reaction is carried out in the pH 4.6 up to target viscosity. When the condition is reached, the 2nd urea is added in order to consume excess of formaldehyde

and determine the F/U mole ratio of final UF resins. After all of the urea dissolve, the UF resins are cooled to room temperature, and the pH is subsequently adjusted to 8.0 for terminating the reaction.

3.6 Modification of Urea Formaldehyde with Nanocellulose

The nanocellulose derived from the combination of baobab pod fibres and waste nose mask material was mixed with urea formaldehyde resin by a way of compounding using two-roll mill shown in Figure 13. The two-roll mill machine was heated to a temperature of 120^{o}C for 30 minutes, which is the melting temperature of the UF resin.

Later on, 90 wt% of UF were poured into the preheated two-roll mill to melt it for about 5 minutes, followed by gradual pouring of 10 wt% cellulose into the melted UF and a complete mixing of the nanocellulose with the UF was done.

Plate VI: Image of a two roll Machine

Finally, the compounded nanocellulose/UF was scraped from the mill and sheet was formed. The resulted compounded sheet was pressed using hydraulic press. At the start, the machine was heated for 30 minutes at the set temperature of 120^{o}C. After which the compounded sample was placed inside a rectangular mould coated with aluminium foil

paper. The arrange mould was taken into the preheated hydraulic press and be held under a pressure of 10 kN for a period of 6 minutes. Thereafter, the samples were removed from the press and allowed to cool before removing the resulting sample from the mould.

3.6.1 Characterization of modified urea formaldehyde

All the samples of the modified UF were tested for their mechanical properties

3.6.1.1 Tensile test

The tensile test was conducted according to ASTM D638 using the Instron universal testing machine. The dimensions, gauge length and cross-head speeds are chosen according to the ASTM D638 standard.

3.6.1.2 Flexural test

Flexural strength was measured under a three-point bending approach using a universal testing machine according to ASTM D790.

3.6.1.3 Impact test

The impact test was conducted according to ASTM D256 using the Charpy V-notch impact testing machine. The dimensions, gauge length and V-notch were chosen according to the standard. The specimen was placed between a special holder with the notch oriented vertically and towards the origin of impact. The specimen was struck by a “tup” attached to a swinging pendulum. The specimen breaks at its notched crosssection upon impact, and the upward swing of the pendulum was used to determine the amount of energy absorbed in the process.

3.6.1.4 Hardness test

The hardness of the polyethylene reinforced baobab fibre composites was measured with the aid of Shore Duro-meter testing machine according to ASTM. The samples were indented following the various fibre compositions in the composites. The reading on the machine was noted and recorded.

3.6.1.5 Water absorption test

The samples to be tested were weighed and submerged in a 250-ml beaker containing water for 24 hrs. After the samples stayed for 24 hrs, then were taken out of the water, dried and weighed according to ASTM D570-98. The percentage water absorbed was calculated using Equation (3.1)

$$M = \_\_\_\_\_ \quad (3.1)$$

Where,

W_0 = the dry weight of the sample

W_t = the weight of the sample after specific time t.

3.7 Fourier Transforms Infrared Spectroscopy (FTIR)

The functional groups of the modified UF samples were determined using Agilent Technologies (Model: Cary 630) FT-IR spectrometer. The specimens were placed on a Kbr plate and inserted into the infrared barrel. The infrared spectra of these samples were measured in the transmission of a wavelength number range between 4500 and 500 cm^{-1}.

3.8 SEM/EDX analysis

Scanning electron microscopy (SEM) machine model Hitachi S3000N VP was used.

Prior to SEM measurements, the samples were coated with a gold layer using an Edwards sputter coater model Pirani 50 I.

3.9 XRD Analysis

X-ray diffraction measurement of samples was carried out using a PANalytical Empyrean X-ray diffractometer with a C_o target, rotating stage and goniometer in 2θ configuration. The wavelength of C_o radiation is 0.179 nm. The generator was utilized at 40 kV and 45 mA. The intensities were measured from 5^o to 110^o at 2θ with step size of 0.0167° and a scan speed of 0.015 deg/sec. The radiation used was full spectrum Co ($K\alpha_1$, $K\alpha_2$) with the K_β filtered out with a diffracted side Fe filter. The empirical Equation 3.2 was used to estimate the degree of crystallinity (crystallinity index, CI) of ground Baobab pod fibres from the XRD results.

$$I_{Cr} = \frac{\quad}{\quad} \times 100 \qquad (3.2)$$

Where

I_{002} is the maximum intensity of the 002 lattice reflection (the highest peak for native cellulose) of the cellulose crystallographic form at $2\theta = 22.5°$

I_{am} is the intensity of diffraction of the amorphous material at $2\theta = 18.5°$

The average crystallite particle size was determined from the XRD patterns of the CNC using Scherer equation represented by Equation 3.3

$$DIV = \frac{\quad}{\quad} \qquad (3.3)$$

Where

D = the particle size diameter

β = the full width at half maximum

λ = the wave length of X-ray

θ = the diffraction angle and K

= the Scherer constant.

CHAPTER FOUR

4.0 RESULTS AND DISCUSSION

4.1 Structural Component of Baobab Fibres

4.1.1 Proximate analysis of raw BPFs

The result for the proximate analysis of raw Baobab pod fibres is shown in Table 4.1. The moisture content of the fibre has a great effect on performance of composites, the higher the moisture content, the more detrimental it is to the performance of composites, it reduces stiffness and flexural strength. Moisture content of 9.4 % for baobab fibres is considered good as compared to other natural fibres. The proximate analysis reveals that, the fixed carbon 71.9 % which is the major component. Amount of ash content have direct correlation with the flexural properties, fixed carbon and volatile matter which indicates the amount of inorganic substituent in the carbon. High ash content is not suitable because adsorption capacity of fibre will be reduced. The low moisture content and low ash content of the Baobab makes it an excellent candidate for urea formaldehyde modification.

Table 4.1: Proximate analysis of raw baobab pod fibres and Waste Nose Mask

Fibre	Moisture (%)	Ash (%)	Volatile Content (%)	Fixed Carbon (%)

Baobab pod and Waste Nose Mask (50:50)	9.4	8.3	9.1	71.9

The results shows that the hybrid material containing a combination of baobab pod fibres and waste nose mask contain higher carbon content when compared to that obtain from corn husk which is 67 % (Kambli et al., 2017), Aloe vera 23 % (Saurabh, 2016) and Marshmallow 70.2 % (Mehmet et al., 2014). Also, the material contains reasonable moisture and ash content when compared to that obtains for Raffia of 11.1 % and 9.2 % respectively (Fadele, 2017).

4.1.2 Ultimate analysis of raw Baobab pod fibres

The value of elemental carbon was consistent with that of the fixed carbon in the proximate analysis. Table 4.2 summarizes the results for the ultimate analysis, it can be seen that the sample consist predominantly of carbon greater than 64 % which indicates a good percentage of cellulose present in the material. Baobab fibres and waste nose mask constitute elements that make it an excellent candidate for composite production.

Table 4.2: Ultimate analysis of Raw Baobab Fibre and Waste Nose Mask

Fibre	Carbon (%)	Hydrogen (%)	Nitrogen (%)	Oxygen (%)
Baobab Pod Fibre and Waste Nose Mask (50:50)	63.6	0.51	16.3	19.6

Table 4.3 shows a comparison of the ultimate analysis of other fibre materials with the hybrid material of waste nose mask. The results indicate that the material consist of elements in percentages that are in percentages similar to those used for composite production

Table 4.3: Comparison of elemental composition of BPF and WNM with other Natural fibres

Material	C	H	N	O	Reference

jackfruit	67.8	1.5	6.8	10.7	Costa et al., 2019
Flax	64.9	-	3.7	8.5	Russo et al., 2020
Pineapple	46.8	-	5.8	4.2	Zwawi, 2021
Bagasse	41.	-	32	12.4	Aliotta et al., 2020

4.2 Fourier Transform infrared (FTIR) Spectroscopy

The Fourier Transform Infrared can be classified in two ways, the finger print group and the function group. Based on the image in figure 4.1, the function group starts with 1500cm^{-1}, then the finger print stars with 1500cm^{-1} - 400cm^{-1}. It is observed from the FTIR spectra in Figure 4.1 that the peak at 1739 cm vibrations due to the aromatic ring presents in lignin and hemicellulose. These aromatics have been effectively removed by the chemical treatment of the baobab pod fibre/waste nose mask. Spectra peaks at 2922 cm, and 2895 cm stretching vibrations of cellulose/hemicelluloses. is ascertained by the reduction of these peaks in as depicted in Figure 16. The FTIR result has established the removal of impurities from the raw fibres resulting in high purity cellulose nanocrystals

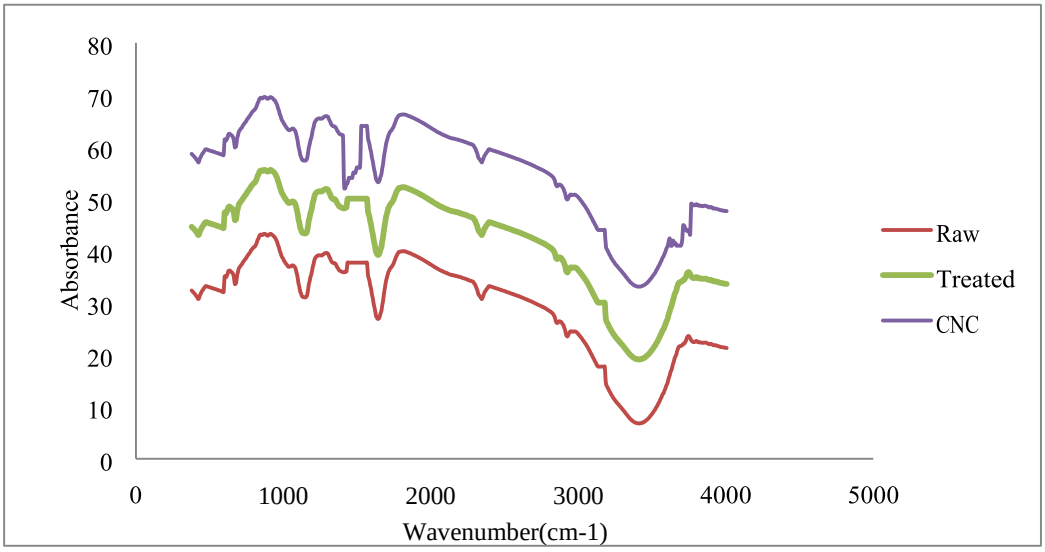

Figure 4.1: FTIR pattern for raw, treated and nanocellulose baobab and waste nose mask

The FTIR spectrum of the nanocellulose displayed absorption patterns corresponding to the specific functional groups of cellulose, and was also in good agreement with the reported cellulose by (Shehu and Iisa, 2017). The peak at 1635 cm^{-1} was formed due to the bending mode of adsorbed water. The peak at 1118 cm^{-1} may be due to CH_2 bending vibration. The sharp transmittance peak around 1384 cm^{-1} represents a bending of OH groups. The peak at 1174 and 1120 cm^{-1} corresponds to C-O asymmetric bridge stretching.

4.3 X-ray diffraction (XRD)

The Cellulose nanocrystals of baobab pod fibres and waste nose mask material as observed from the XRD results is shown in Figure 4.2. 2θ peaks were observed at 15.32, 22.02, corresponding to (1$\bar{1}$0), (020), Miller indices as in cellulose I. The presence of cellulose II in the NCCs is evident by the peaks at 20.77º. Cellulose I structure is established by the peaks at 22.02. The formation of cellulose two (II) is due to acids treatment. The crystallinity index of the cellulose nanocrystals as calculated from equation (3.2) is 91%. The C.I value obtained in this work falls within close range as reported from previous literature. The XRD result reveals the transformation of cellulose I to II and high C.I compared with the source material.

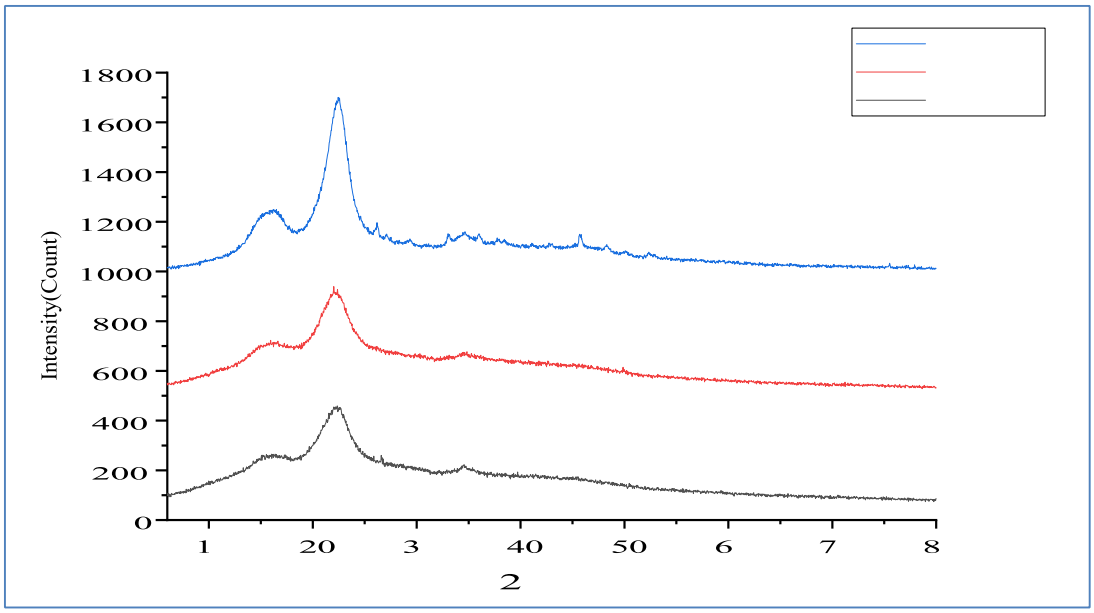

Figure 4.2: X-ray diffraction pattern of Cellulose Nanocrystals of Baobab & Waste Nose Mask

The nanocellulose exhibited a typical cellulose I pattern at a sharp peak of 2θ =22°. The diffraction peak at 22° corresponds to the 002 crystallographic plane of the cellulose I lattice. The crystallinity index (CrI) was calculated according to the Segal empirical method.

4.4 SEM for Raw Baobab Pod Fibre and Waste Nose Mask

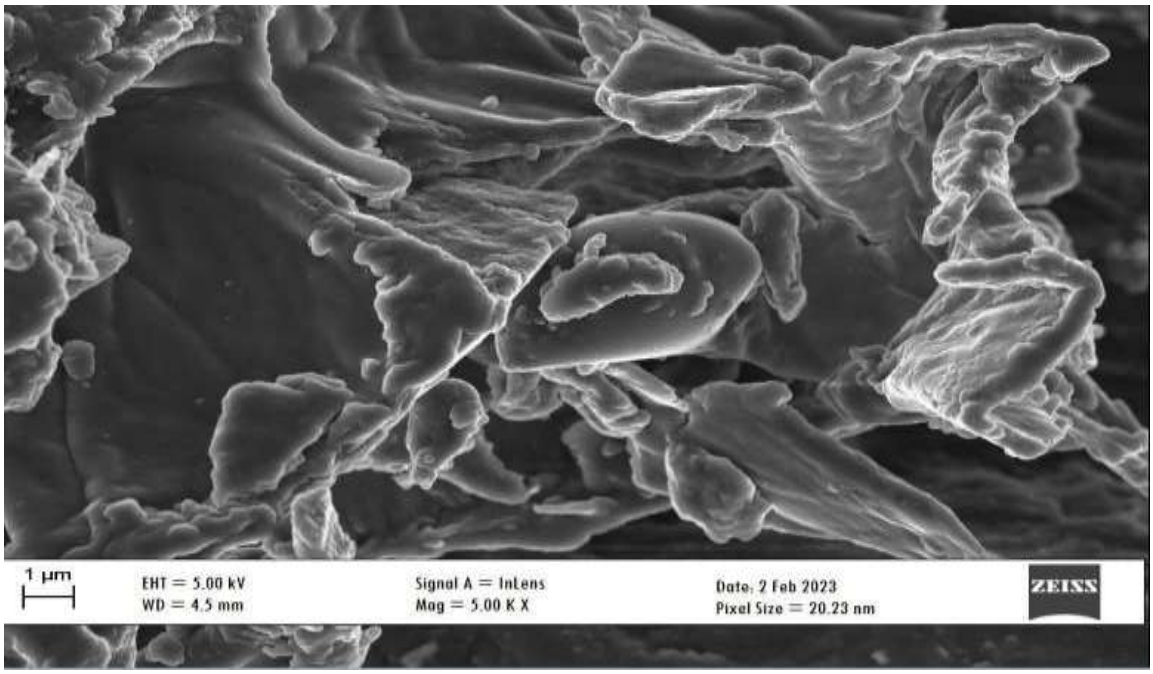

Figure 4.3: SEM images of Raw Baobab - Waste Nose Mask

The SEM shown in Figure 4.3 indicates three distinct regions: an inner region (lumen), a middle region (cortex) and an outer surface (epidermis). Between the outer surface and the inner core, there are radial pathways, which probably serve as conduits for water/moisture exchange between the core of the fibre and the environment. The spectrum shows voids in the material, the cross-sectional structure is almost similar to the reported structure of several natural fibres like, Rafia (Fadele, 2017), coir fibres (Tan et al., 2015) and sisal fibre (Ernestina et al., 2013). The surface morphology consisted of an amorphous phase of lignin and hemicelluloses covering the cellulose microfibrils.

4.5 SEM for NaOH Treated Baobab Pod Fibres and Waste Nose Mask

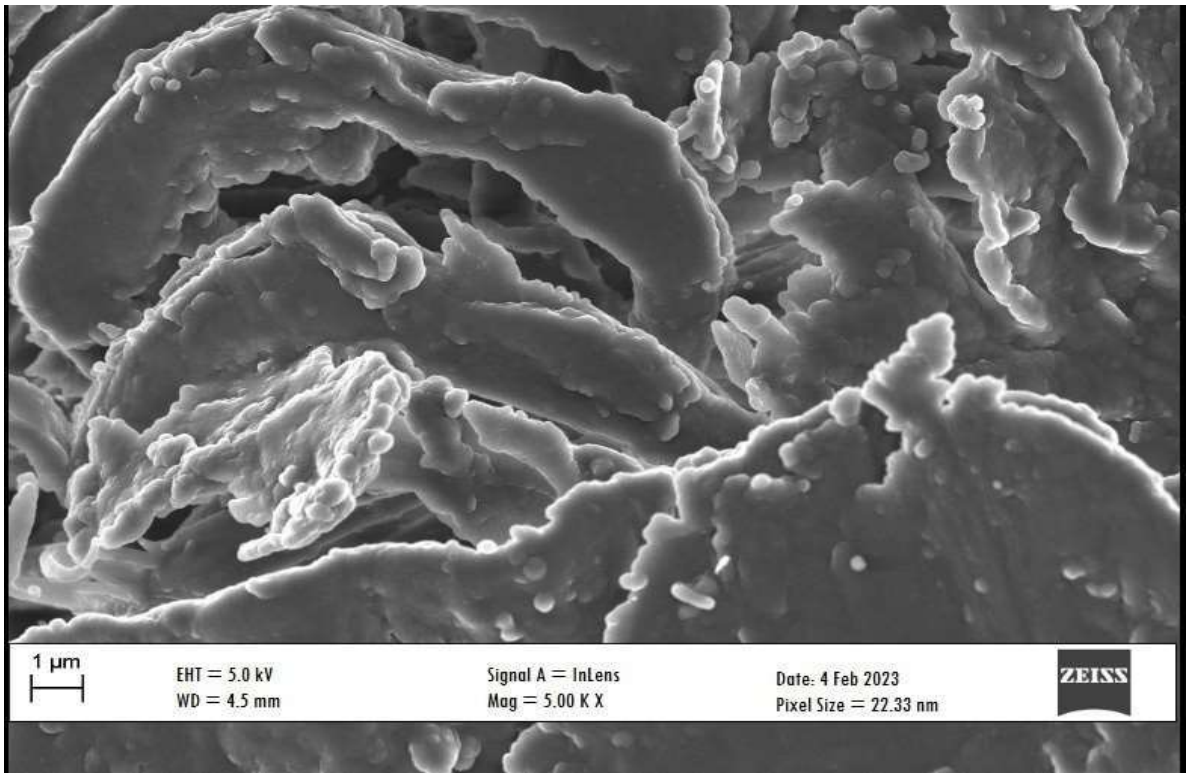

Figure 4.4: SEM images of treated Baobab - Waste Nose Mask

The chemical treatment leads to significant changes in the fibre surface morphology. The surfaces of alkali treated BPFs appear to be much clearer than those of raw fibres as shown in Figure 4.4. This indicates that Sodium Hydroxide removed oil, wax and other impurities from the surfaces of the fibres. The use of chemical treatment on natural fibres results in the removal of non-cellulose components and also resulted in changes in both thermal properties and surface chemistry of natural fibres. The removal of these materials is expected to promote strong bonding between the fibre and the polymer matrix when used in composite manufacture (Kabir et al, 2012).

4.6 SEM for Baobab Pod Fibre and Waste Nose Mask Nanocellulose

SEM was employed to analyse the structure of nanocrystals of the cellulose formed. The SEM images in Figure 20 indicate changes in morphology of the nanocellulose.

The nanocrystals have tiny rod like shapes and some spherical in shape. The features of the cellulose nanocrystal in the nanocellulose showed that there was a reduction in the fibrillar structure size and intermittent breakdown in fibrillar structure into individualised fibrils.

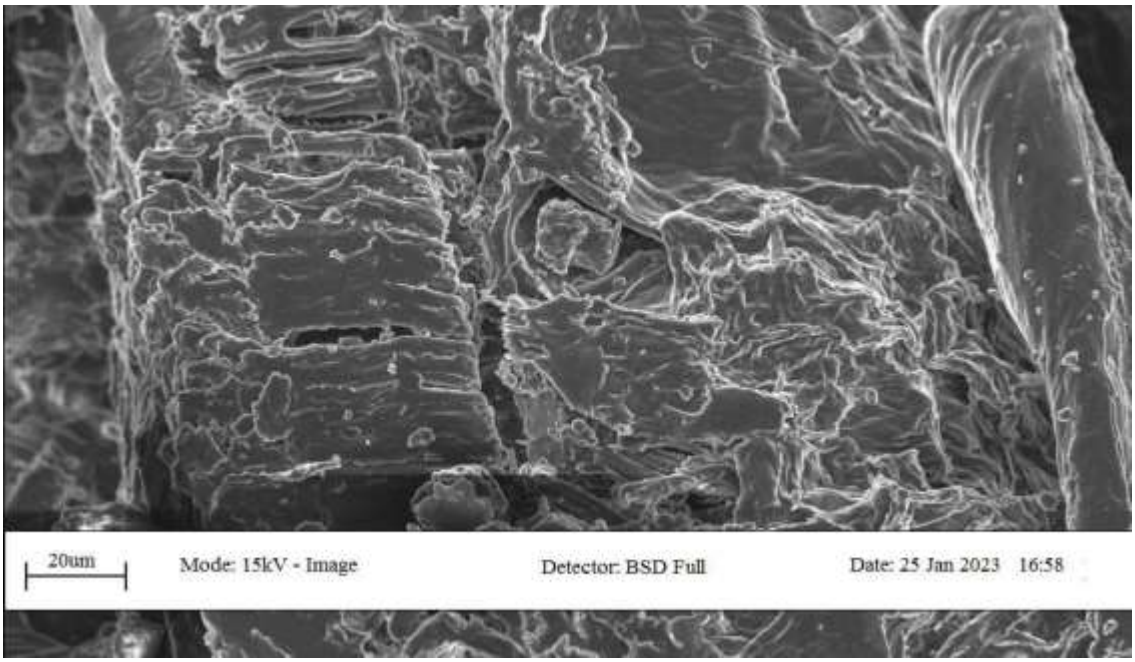

Figure 4.5: SEM images of Cellulose Nanocrystals of Baobab - Waste Nose Mask

4.7 Characteristics of Synthesised Urea Formaldehyde

Table 4.4 showed the characteristics of UF resins synthesized in this work. Reducing the F/U mole ratio resulted in increasing of solid content of the resin due to the addition of the second urea used in raw materials. Moreover, there was a tendency of the density; the lower F/U mole ratio of UF resin the higher of the density. UF resin with the lowest F/U mole ratio gave the highest density probably because of the sol fraction containing in the resin.

Previous work on film UF resin exhibited abundant sol fraction in low F/U mole UF resin compare to in high F/U mole UF.

Table 4.4: Characteristics of Synthesized UF Resins

Sample	F/U mole ratio	Solid Content (%)	Density (g/cm^3)	Viscosity (MPa.s)	Gel time (min)	Colour
Neat	0.94	51.6	1.53	214	13.12	Dispersed, milky white
UF1	1.04	47.61	1.47	143	11.47	Black
UF2	1.14	46.8	1.46	130	9.43	Black
UF3	2.01	37.9	1.45	443	4.42	Black
UF4	2.03	36.1	1.41	449	3.99	Black

The trend showed the highest F/U mole ratio of UF resin has had the most viscous, indicating that the reactivity of high F/U mole ratio UF resin adhesive was greater compared to that of the low F/U mole ratio. A lower viscosity indicated a low molecular weight of UF resin adhesives because the viscosity of liquid UF resin adhesives is proportional to their molecular weight. Related to gel time measurements, indeed UF resin with high F/U mole ratio was more reactive contrasted by low F/U mole ratio. The milky white colour of the resin is due to ageing or further advancement of the resin by condensation reaction.

4.8 Characterization of Modified Urea Formaldehyde with Baobab and Waste Nose Mask Nanocellulose

Various characterization methods were carried out on the modified urea formaldehyde baobab/waste nose mask nanocellulose in order to determine how effective it will be when applied in use as an engineering material. Some of the characterization methods used includes;

4.8.1 Water absorption properties of modified urea formaldehyde resins

This test method for rate of water absorption has two chief functions: first, as a guide to the proportion of water absorbed by a material and consequently, in those cases where

the relationships between moisture and electrical or mechanical properties, dimensions, or appearance have been determined, as a guide to the effects of exposure to water or humid conditions on such properties and secondly, as a control test on the uniformity of a composite. Figure 4.6 shows the results of water absorption properties of urea formaldehyde on varying baobab/nose mask nanocellulose loading. The water absorption capacity increased with increasing cellulose nanocellulose loading.

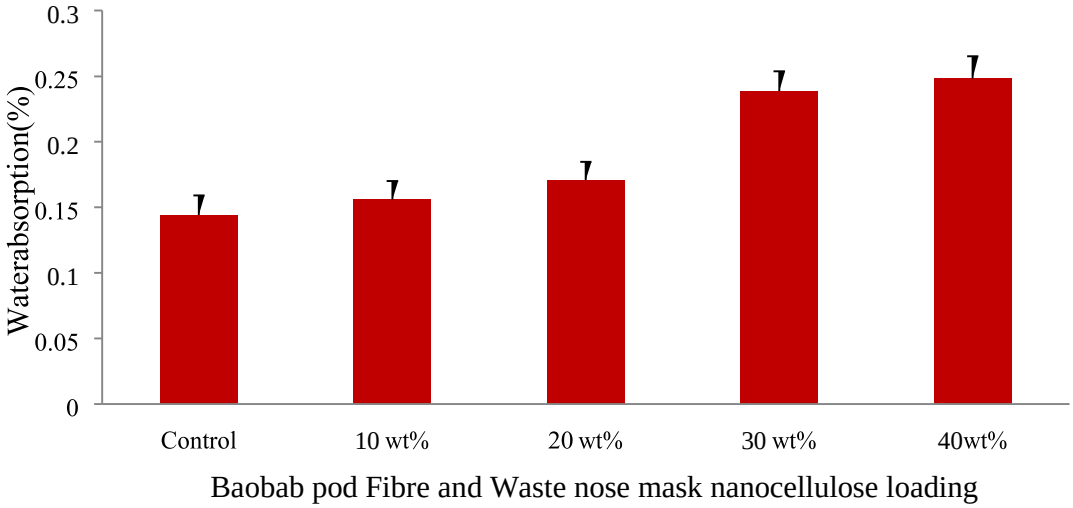

Figure 4.6: Water absorption capacity % of modified urea formaldehyde resins

4.8.2 Tensile properties of modified urea formaldehyde resins

Tensile strength is one of the most important properties of nanocellulose reinforced composites because it indicates the resistance of material to break under tension. Figure 4.7 shows the maximum tensile strength for the modified urea formaldehyde to be 86 MPa for 30 wt % which is much higher than that of the virgin (unmodified) resin which has 61 MPa.

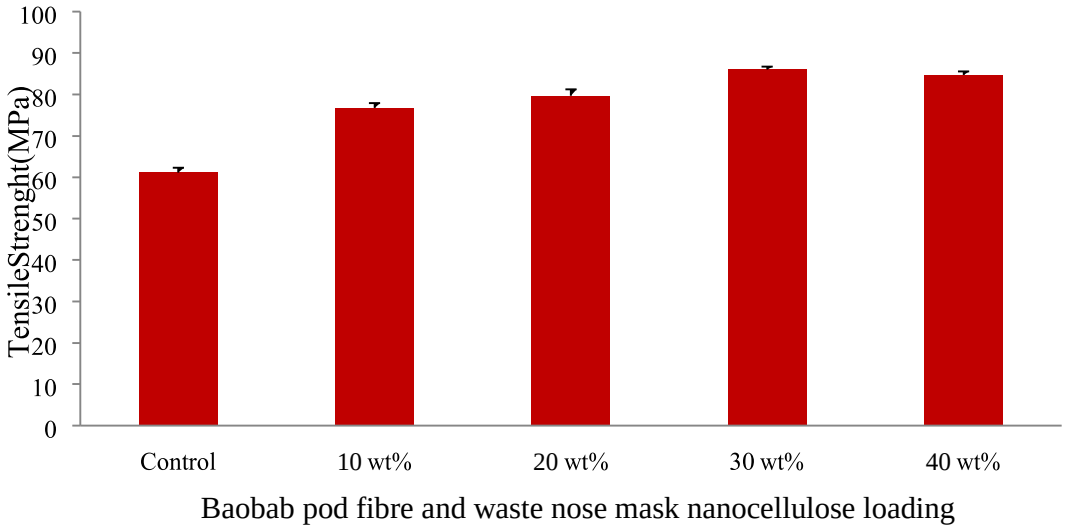

Figure 4.7: Tensile Strength of modified urea formaldehyde resins

The maximum tensile strength obtained at 30 wt% might be due to proper binding between the urea formaldehyde and he nanocellulose obtained from baobab and waste nose mask. It can be observed that all the modified samples had tensile strength higher than that of the unmodified (control) sample.

4.8.3 Flexural strength of modified urea formaldehyde resins

The flexural strength of the modified samples is higher than that of the unmodified (control) sample as shown in Figure 4.8. This is a clear indication that flexural strength was increased with baobab/waste nose mask addition. The highest flexural strength was obtained at 30 w % which is 17.36 MPa. The overlap in error bar between 20 wt %, 30 wt % and 40 wt % does not show much significant difference between the results.

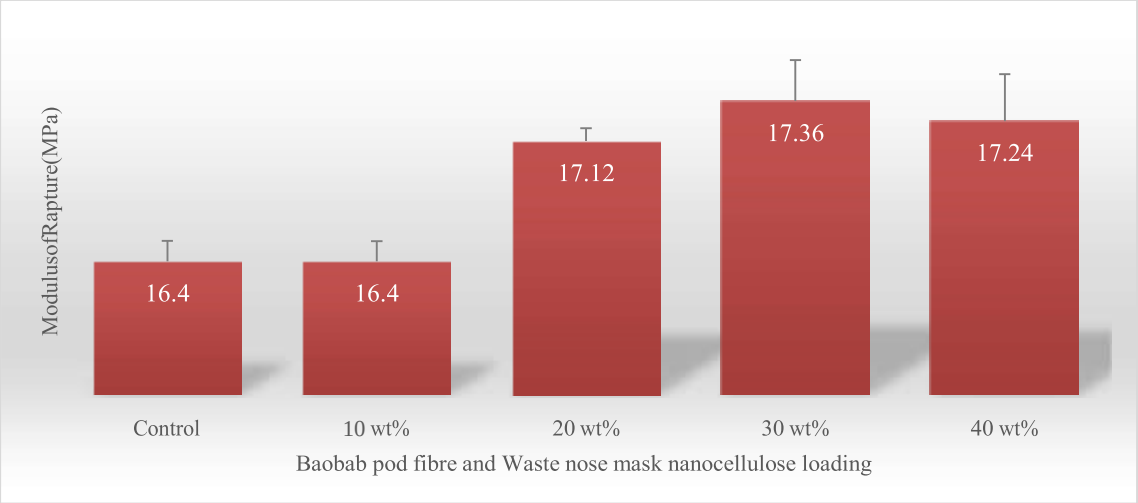

Figure 4.8: Flexural strength of modified urea formaldehyde resins

All samples have modulus of rapture above 16.4 MPa while that of the unmodified sample stood at 16.4 MPa this shows that the unmodified sample has the tendency to rapture faster than that of the modified samples.

4.8.4 Hardness properties of modified urea formaldehyde resin

Figure 4.9 shows that the addition of the nanocellulose to the urea formaldehyde increases the hardness property, this indicated that hardness of the modified material is directly proportional to the increase in baobab/waste nose mask nanocellulose addition. The lowest hardness strength of 26.7 HV was obtained at 10 wt% of nanocellulose loading while the highest was recorded at 45.3 HV for 40 wt %

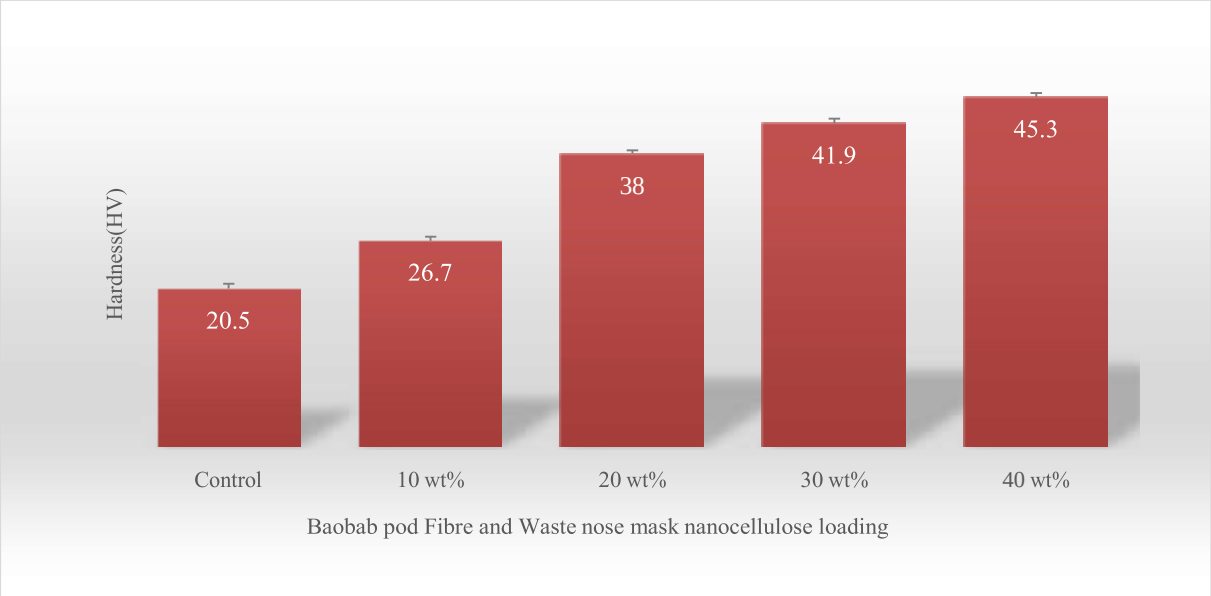

Figure 4.9: Hardness of modified urea formaldehyde resins

4.8.5 The effect of impact strength on modified urea formaldehyde resins The impact strength of the modified urea formaldehyde decreased with increased loading of baobab/waste nose mask nanocellulose as can be seen from Figure 4.10. The impact properties decrease due to poor interfacial adhesion between the binding materials. The nanocellulose loading increases the brittleness of the modified material. The error bar overlapped between 10 wt %, 20 wt% and 30 wt% nanocellulose loading shows that there was no significant change in impact strength between the two modified samples.

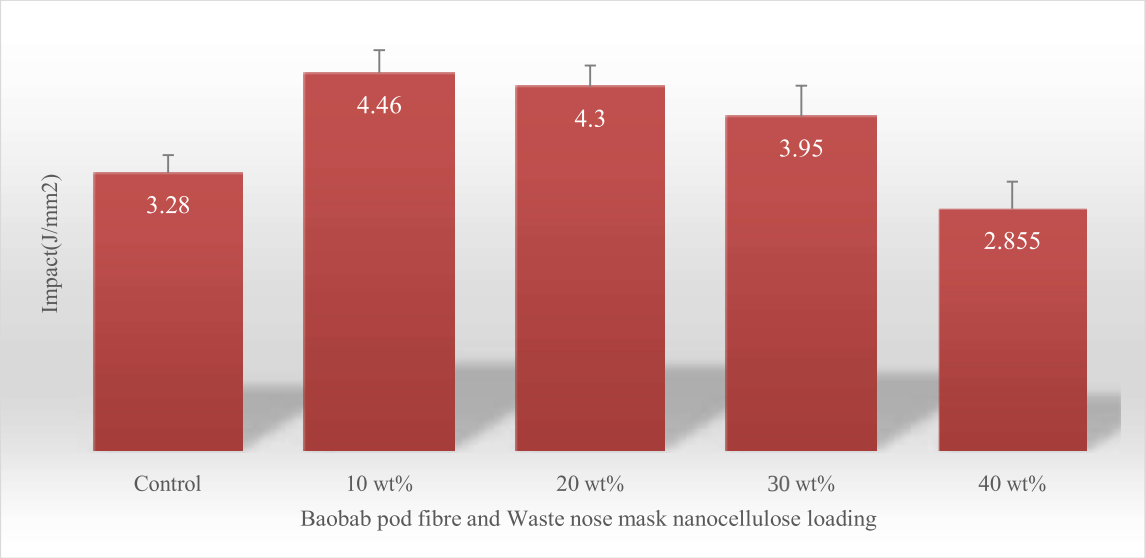

Figure 4.10: Impact Strength of modified urea formaldehyde loading

4.9 FTIR Analysis of Neat Urea formaldehyde

FTIR spectrum of the neat urea formaldehyde (UF) showed characteristic peak at 3290 cm^{-1} (N–H stretching peak of primary amines), 2926 cm^{-1} and 2854 cm^{-1} (C–H stretching of UF), 1656 cm^{-1} (C=O stretching vibration), 771 cm^{-1} (N– H bending of secondary aliphatic amines). The absorption band at 1381cm^{-1} and 1028 cm^{-1} is due to N–C–N and C– N stretching of methylene linkage (NCH_2N) of amides in resin (Park and Jeong, 2011).

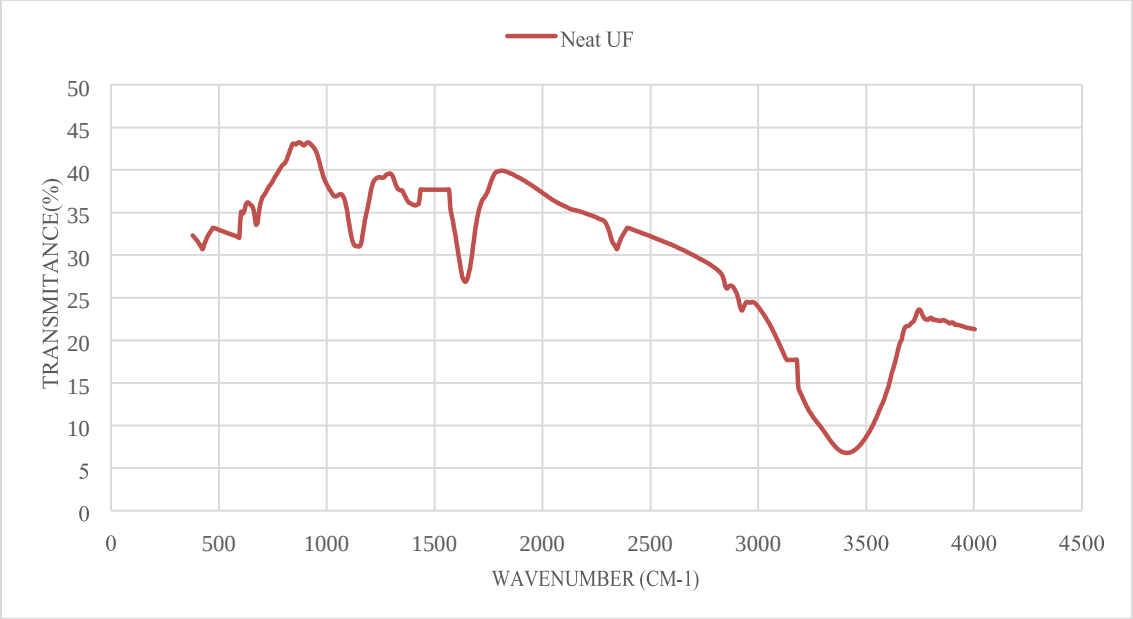

Figure 4.11: FTIR analysis of neat urea formaldehyde

4.10 FTIR Analysis of Modified UF Resins

The comparable band intensities and peak positions in FTIR spectra of baobab/waste nose mask nanocellulose suggest the similar chemical composition and significantly high cellulose content in both of the fibres. The absorption peaks corresponding to both UF and fibres observed in FTIR spectra of the modified UF composite suggest the uniform distribution of the nanocellulose in the matrix in composite system. The absorption bands in composite at 3280 cm^{-1} was due to O–H stretching vibration. The shifting at 2926 cm^{-1} to 2960 cm^{-1} for C-H stretching peak suggests that $–CH_2$ group of the cellulose played significant role in nanocellulose and matrix interfaces. Similar small peak shifts in FTIR spectra between 1000 cm^{-1} to 1750 cm^{-1} represents the weak chemical interaction in filler and matrix (Zorba et al. 2008).

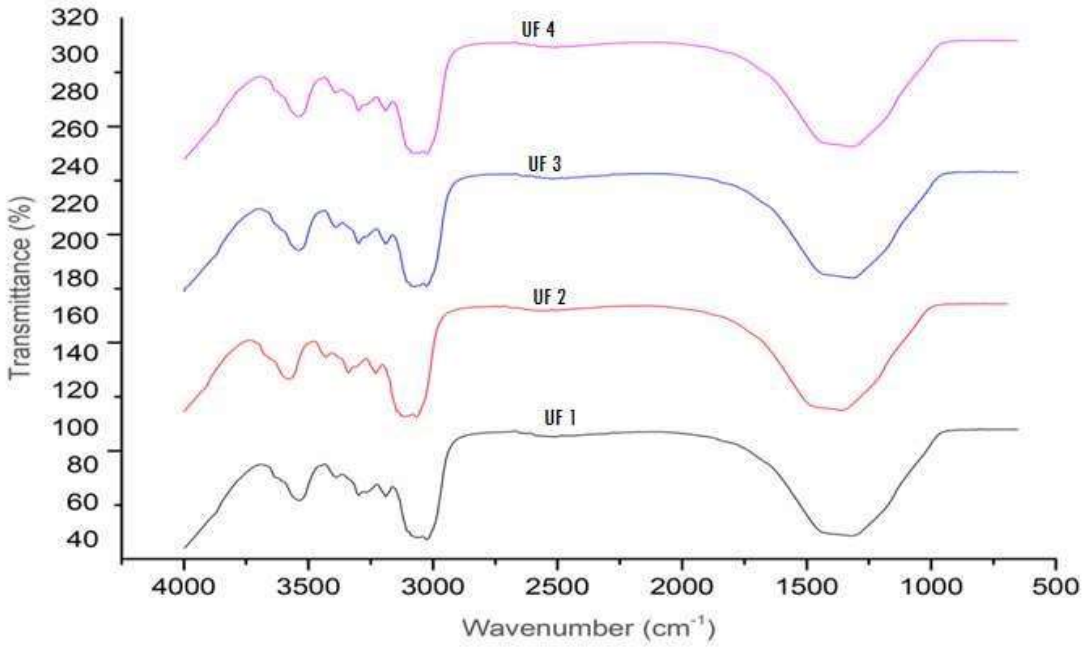

Figure 4.12: FTIR analysis of modified urea formaldehyde samples

4.11 SEM Analysis for Modified Urea Formaldehyde

Figures 4.13 represent SEM micrograph of the modified UF composites with baobab and waste nose mask and of 90/10 (UF 1) composition by weight percent.

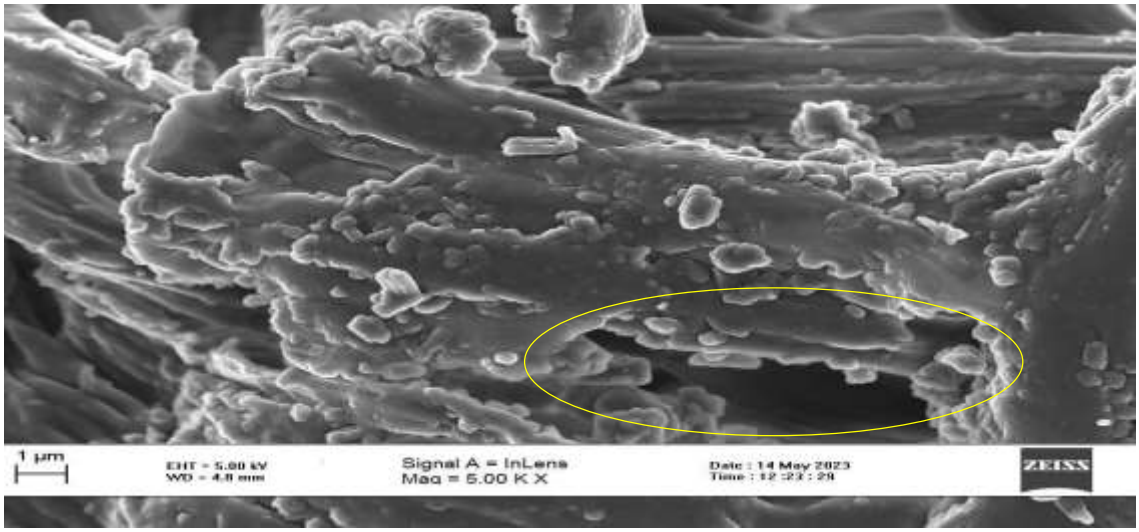

Figure 4.13: SEM spectrum of modified UF resins

Although the nanocellulose are homogeneously distributed in the UF matrix, the appearance of dark voids and gaps around the nanocellulose–matrix interface implies their non compatibility with polymer matrix.

4.12 TGA Analysis for Neat Urea Formaldehyde

From the TGA curve shown in Figure 4.14, Small mass loss between 150- 200° C is attributed to slow release of free formaldehyde from UF and that between 220- 250° C is attributed to degradation of methylene ether bridges in the resins network. The major pyrolysis process of pure UF takes place between 270- 350° C, maximum being at 292° C. The last stage that occurs above 350° C is the further pyrolysis process of a thermally stable residues formed in the former stage with slight weight loss leading to about 15 % of final residual mass.

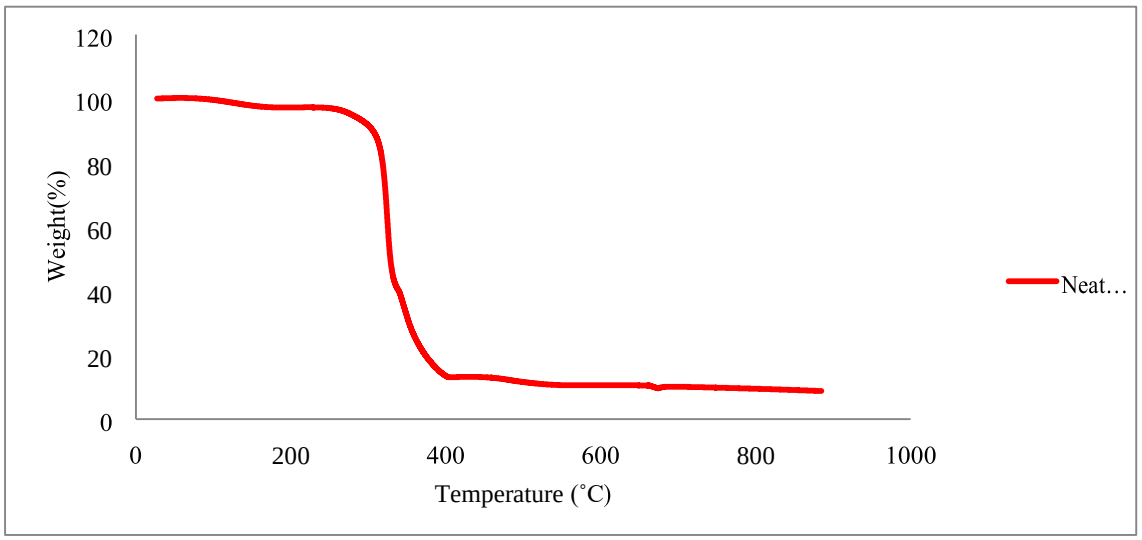

Figure 4.14: TGA of Neat UF Resin

4.13 TGA Analysis for Modified Urea Formaldehyde

Fig. 4.15 represents the derivative of TGA curve of the baobab pod fiber and waste nose mask nanocellulose modified UF resin the curve shows that the thermal degradation of natural fibres is a two-step process, below 100° C was due to release of volatiles and

moisture present in the fibre and other in between 250- 450° C was due to decomposition of lignin, hemicellulose and cellulose of the fibres. Specifically, with UF1 and UF2, weight loss between 250- 300° C was due to thermal decomposition of hemicelluloses and break of glycoside linkage in cellulose molecules. The maximum mass loss appeared between 350- 400° C. The low-temperature degradation process was associated with degradation of hemicellulose whereas the high-temperature process was due to lignin.

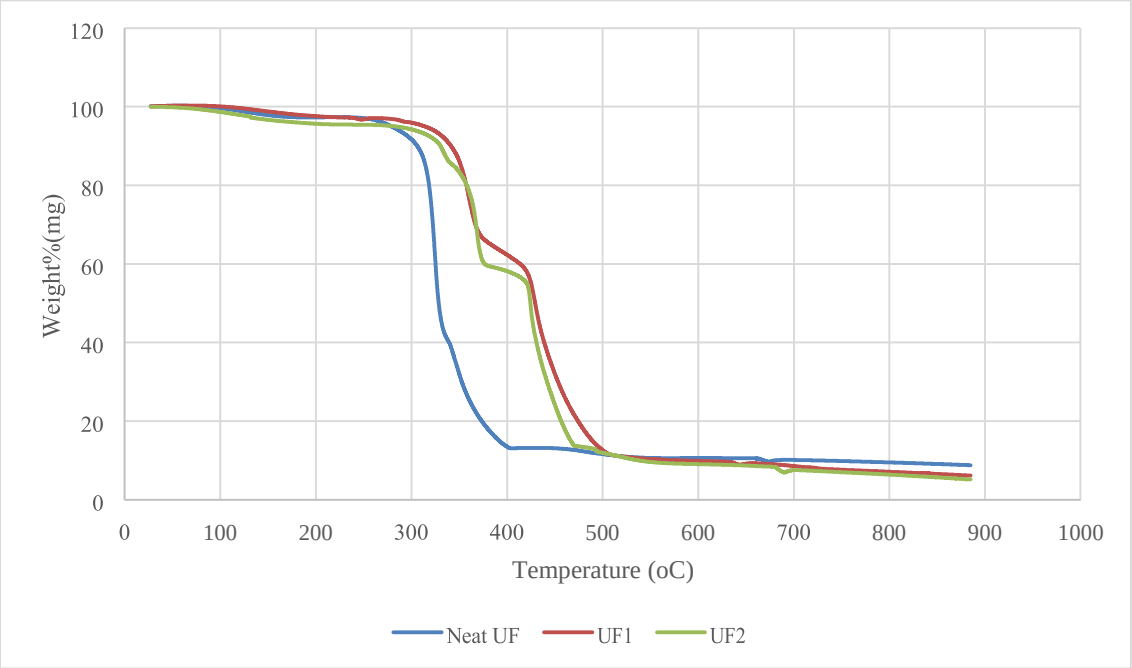

Figure 4.15: TGA of modified UF Resin, UF1 and UF2

Table 6 shows the comparison of the maximum working temperatures for baobab and waste nose mask modified UF composites with other composites

Table 4.5: Comparison of maximum working temperatures for baobab /waste nose mask modified UF composites with other composites

Sample	Maximum working temperatures (˚C)	Reference
UF & BPF/WNM	220	This study
Epoxy & kenaf fibre	200	Chan et al., 2013
Sisal & interlamina	180	Mwaikambo et al., 2002
Raffia & HDPE	210	Fadele, 2017
Wiskers & PE	232	Azizisamir et al., 2015

From table 4.5, it shows that the modified urea formaldehyde and baobab fibre//waste nose mask material composite has higher working temperatures that others listed. This shows that it can be used in applications where higher temperatures are required.

CHAPTER FIVE

5.0 CONCLUSION AND RECOMMENDATIONS

5.1 Conclusions

In this investigation, the potentiality of baobab pod fibres and waste nose mask for urea formaldehyde resin modification was studied. Conclusions from this study are as follows:

1. A nanocellulose composite was produced from Baobab pod fibres mixed with nose mask, they contained high cellulose content which is the most important structural component in plant natural fibre.
2. Characterization analysis was done on the nanocellulose composite to confirm if the composite was suitable for the study.
3. The urea formaldehyde was modified with the addition of the nanocellulose composite containing baobab pod fibre and nose mask materials.
4. Characterization analysis was carried out on the modified urea formaldehyde with the nanocellulose composite of Baobab pod fibres with nose mask. The nanocellulose composite can be used for urea formaldehyde resin modification because of its high crystallinity index. High crystallinity means that the fibres will have relatively low amorphous region which increases the amount of moisture absorbed in natural fibres.
5. Good tensile properties will increase mechanical performance when used to modify urea formaldehyde resins.

From the present investigation it can further be concluded that properties of baobab pod fibres make it a strong candidate with good potential to be used as modification for urea formaldehyde resins which can be use in various applications.

5.2 Recommendation

The following recommendation should be noted

1. Further research should focus on the application of the modified urea formaldehyde
2. Other natural fibres should also be used for modifying other polymers
3. Other matrix should also be used with baobab fibre.
4. Response surface methodology (RSM) method can be used to optimize the chemical treatment conditions

5.3 Contribution to Knowledge

The present study made a significant contribution to the knowledge and understanding of modifying urea formaldehyde (UF) resin using nanocellulose derived from baobab pod fiber and waste nose mask. Here are the key contributions:

This study explored the novel application of nanocellulose derived from unconventional sources, namely baobab pod fiber and waste nose mask, for modifying UF resin. This application opens up new possibilities for utilizing sustainable and eco-friendly materials in the composite industry.

The study also provides a comprehensive characterization of baobab pod fiber and waste nose mask fibers, including their properties and chemical treatment to improve adhesion. This characterization enhances our understanding of the suitability of these fibers for nanocellulose production.

The research employs acid hydrolysis to produce nanocellulose from the treated fibers.

The investigation of functional groups, surface morphology, and crystallinity using advanced analytical techniques such as FTIR, SEM/EDS, and X-ray Diffraction contributes to the knowledge of nanocellulose synthesis and its properties.

The study evaluates the mechanical properties of Urea Formaldehyde resin modified with nanocellulose at different ratios. The findings demonstrate the positive impact of nanocellulose on enhancing the tensile strength, modulus of elasticity, and elongation at break of the modified resin. This knowledge contributes to the development of highperformance and sustainable composite materials.

By utilizing waste nose masks and exploring biodegradable alternatives, the research addresses environmental concerns associated with formaldehyde emissions and nonbiodegradable plastics. This contribution aligns with the global efforts to reduce pollution and promote sustainable practices in the composite industry.

REFERENCES

Aliotta, L., Vannozzi, A., Panariello, L., Gigante, V., Coltelli, M-B., & Lazzeri, A., (2020). Sustainable Micro and Nano Additives for Controlling the Migration of a Biobased Plasticizer from PLA-Based Flexible Films. Polymers, 12(6), 1366; https://doi.org/10.3390/polym12061366s

Anteneh G., Tamene A. D., Pieter, D. W. & Hans, D. B. (2021). An Overview of the Characterization of Natural Cellulosic Fibre. Article in Key Engineering Materials DOI: 10.4028/www.scientific.net/KEM.881.107. ISSN: 1662-9795, Vol. 881, pp 107-116

Antov, P.; Savov, V.; & Neykov, N. (2020). Reduction of Formaldehyde Emission from Engineered Wood Panels by Formaldehyde Scavengers—A Review. In Proceedings of the 13th International Scientific Conference Wood EMA 2020 and 31st International Scientific Conference ICWST, Vinkovci, Croatia, 28–30 September 2020.

Arun, K. S., Rakesh, B., Amit, A. & Ruta, R. (2020). A study of advancement in application opportunities of Aluminium metal matrix composites. Materials today proceedings (10) 2214-2215

Budhi, Y.W., Fakhrudin, M., Culsum, N.T.U., Suendo, V., & Iskandar, F. (2018) Preparation of cellulose nanocrystals from empty fruit bunch of palm oil by using phosphotungstic acid. IOP Conf. Series: Earth and Environmental Science 105 (2018) 012063 doi :10.1088/1755-1315/105/1/012063

Chieng, B. W., Lee, S. H., Ibrahim, N. A., Then, Y. Y., & Loo, Y. Y. (2017). Isolation and characterization of cellulose nanocrystals from oil palm mesocarp fiber. Polymers, 9(8), 355.

Choong, H. Cui, Y. Liu, X. Zhang, M. Hao, S. & Yin, Y. (2019). Study on depositing SiO_2 nanoparticles on the surface of jute fibre via hydrothermal method and its reinforced polypropylene composites. Journal of Vinyl Additive Technology. 26, 43–54

Chattopadhyay, D. (2004) Life-Cycle Maintenance Management of Generating Units in a Competitive Environment. IEEE Transactions on Power System, 1181-1189. http://dx.doi.org/10.1109/TPWRS.2003.821616

Damfeu, J. C., Meukam, P. & Jannot, Y (2016). Modeling and measuring of the thermal properties of insulating vegetable fibres by the asymmetrical hot plate method and the radial flux method: Kapok, coconut, groundnut shell fibres and rattan. Thermochimical Acta , 630, 64–77

De Caluwe, E., Katerina, H. & Patrick, V.M. (2010). Adansonia digitata L. – A Review of Traditional uses. Phytochemistry and pharmacology. Afrika Focus – 23,11-51

Dipen K.R., Pradip M., Durgesh, P. & Emanoil, L. (2019). Fibre-Reinforced Polymer Composites: Manufacturing, Properties, and Applications. MDPI Polymers. (11), 1667; doi:10.3390/polym11101667

Dunky, M., Gavrilovic-Grmusa, I., Miljkovic, J. & Djiporovic-Momcilovic, M. (2012). Influence of the viscosity of UF resins on the radial and tangential penetration into poplar wood and on the shear strength of adhesive joints. Holzforschung, 66(7), 849-856. https://doi.org/10.1515/hf-2011-0177

El Achaby M, El Miri N, Hannache H, Gmouh S, Ben Youcef H, & Aboulkas A. (2018) Production of cellulose nanocrystals from vine shoots and their use for the development of nanocomposite materials. Int J Biol Macromol 1;117:592600.doi:10.1016/j.ijbiomac.2018.05.201.

Fadele., O.E., (2017). Development and Characterization of Raffia Palm Fiber Reinforced Polymer Matrix Composites (Unpublished Doctoral Dissertation). University of Saskatchewan. Saskatoon

FAO (1988). Traditional food plants. Food and Agriculture Organisation of the United Nations;Rome, 24: 63-67.

Faridulhassan, K.M., Horváth, P.G., & Alpár, T. (2020). Potential Natural Fiber Polymeric Nanobiocomposites: A Review. Polymer. 12(5):1072 http:/doi.org/10.3390/polym12051072

Gebauer, M. P. (2010). Fundamentals of Modern Manufacturing: Materials, Processes, and Systems. John Wiley Sons, Incoporated Danvers, Massachusetts, USA, 4, 1025.

Harshai, P., Vjay, S. & Pramod, R. (2019). Characterization of natural fibre reinforced polymeric composites for automotive application - a review. An article on technical textiles.www.researchgate.net/publication/33199170

Hastuti, N., Kanomata, K. & Kitaoka, T. (2018)Hydrochloric Acid Hydrolysis of Pulps from Oil Palm Empty Fruit Bunches to Produce Cellulose Nanocrystals. J Polym Environ 26, 3698–3709. https://doi.org/10.1007/s10924018-1248-x

Hazrol, M. D., Spuan, S. M, Zuhri, M. Y. M. & Ilyas, R. A. (2019). Eletrical properties of sugar palm nanocellulose fibre reinforced sugar palm starch biopolymer composite. In proceeding Semina Enau Kebangsaan pp 2 - 11

Idowu, D. I., Tamba, J. & Gbenga, E. (2016). Mechanical properties of sisal fibrereinforced polymer composites: a review. Composite Interfaces. Vol.23, Issue.No.1, pp. 15–36.

Igboeli, L.C., Addy, E. & Salami, L. I. (1997). Effects of some processing techniques on the antinutrient contents of Baobab seeds (Adansonia digitata). Bio resource Technology 59: 29-31.

Islam, A, Okano, T. & Sugiyama, J. (2013). Fine structure and tensile properties of ramies in the crystalline form of cellulose I, II, III and IV'. Polymers 38(2): 463 – 8.

Jacob, J. O., Kakulu, S. E., Paiko, Y. B., Adeyemi, H. R.Y., & Ndamitso, M. M. (2004). Determination Of Bioavailable Concentrations of Copper and Zinc in Farm Soils in Kaduna Metropolis, Nigeria. Ife Journal of Science vol. 17, no.

1. Pg 229-237

Kabir, M.M., Wang, H. Lau, K.T., & Cardona, F. (2012). Chemical treatments on plant-based natural fibre reinforced polymer composites: An overview. Composites Part B: Engineering. 43. 2883–2892. 10.1016/j.compositesb.2012.04.053.

Kambli, N.D., Mageshwaran, V., & Patil, P.G. (2017). Synthesis and characterization of microcrystalline cellulose powder from corn husk fibres using bio-chemical route. Cellulose 24, 5355–5369. https://doi.org/10.1007/s10570-017-1522-4

Kolibaba, O., Sokolsky, A & Gabitov, R. (2017). Investigation of solid organic waste processing by oxidative pyrolysis. Journal of Physics: Conference Series. 891. 012117. 10.1088/1742-6596/891/1/012117.

Leja, K. (2010). Polymer Biodegradation and Biodegradable. Polish Journal of Environmental Studies, 255 - 266.

Miyashiro D, Hamano R, & Umemura K. (2020). A Review of Applications Using Mixed Materials of Cellulose, Nanocellulose and Carbon Nanotubes. Nanomaterials.; 10(2):186. https://doi.org/10.3390/nano10020186

Mohammed, L. Ansari, M. N. M. Pua, G. Jawaid, M. & Islam, M. S. (2015). A Review on Natural Fibre Reinforced Polymer Composite and Its Applications. International Journal of Polymer. doi:10.1155/2015/243947.

Mohammed Z. (2021). A Review on Natural Fibre Bio-Composites, Surface Modifications and Applications. Journal of Molecules 26, 404. https://doi.org/10.3390/molecules 26, 20 - 40

Mohanty, A. K., Misra, M. & Hinrichsen, G. (2000). Biofibres, biodegradable polymers and biocomposites: an overview. Macromol Material Engineering 276–277:1–24

Nguyen, T.A. Han, B. Sharma, S. Longbiao, L. & Bhat, K. S. (2020). Fibre-reinforced nanocomposites: An introduction. In Fibre-Reinforced Nanocomposites: Fundamentals and Applications. Elsevier BV: Amsterdam, The Netherlands, 3–6

Niddles, H. L., (2001). Textile fibres, dyes, finishes and process. Special publishers Distributors.67, 89-90.

Nissen, D. & Stutz, H. (1985). Advanced Composite Matrices CCM Annual Workshop, Centre for Composite Materials. University of Delaware, Newark. Del. 19, 7-16.

Park, B.-D.; Jeong, H.-W. Hydrolytic (2011) Stability and Crystallinity of Cured Urea–Formaldehyde Resin Adhesives with Different Formaldehyde/Urea Mole Ratios. Int. J. Adhes. Adhes. 2011, 31, 524–529.

Peets, P., Leito, I., Pelt, J. & Vahur, S. (2017). Identification and classification of textile fibres using ATR-FT-IR spectroscopy with chemometric methods. Spectrochim Acta Molecular Biomolecular Spectroscopy.; 15(173):175–81

Russo, P.,Vitiello, L., Sbardella, F., Santos, J. I., Tirillò, J., Bracciale, M. P., Rivilla, I., & Sarasini, F. (2020). Effect of Carbon Nanostructures and Fatty Acid Treatment on the Mechanical and Thermal Performances of Flax/Polypropylene Composites. Polymers. 12, 4-38

Shehu, U. & Isa, M. T. (2017). Effects of NaOH modification on the mechanical propertiesOf Baobab pod fibre reinforced LDPE composites. Nigerian Journal of Technology (NIJOTECH), 36, 87 – 95.

Shetty AJ, Choudhury D, Rejeesh, Nair V, Kuruvilla M, & Kotian S. (2010) Effect of the insulin plant (Costus igneus) leaves on dexamethasone-induced hyperglycemia. Int J Ayurveda Res.;1(2):100-2. doi: 10.4103/09747788.64396. PMID: 20814523; PMCID: PMC2924971.

Tan, B., Ching, Y., Poh, S., Abdullah, L. & Gan, S. (2015). A Review of Natural Fibre Reinforced Poly (Vinyl Alcohol) Based Composites: Application and Opportunity. Polymers (Basel) 7, 2205–2222

Tokiwa, Y., Calabia, B., Ugwu, U., & Aiba, S. (2009). Biodegradability of Plastics. International journal of molecular sciences. 10. 3722-42. 10.3390/ijms10093722.

Tomita, B. &Hatono, S., (1978) Urea – formaldehyde resins. III, J. Polym. Sci. 1978, 16, 2509 – 2525.

Ubi, P. A. & Abdulrahman, S. A. (2015), Effect of Sodium Hydroxide Treatment on the Mechanical Properties of Crushed and Uncrushed Luffa Cylindrical Fibre Reinforced LDPE Composites. International journal of chemical, Nuclear, Material and Metallurgical Engineering. 9, (1), 203-208

Venter, F. & Venter, J.(1996). Baobab in Making the Most of Indigenous Trees. Briza publications, Pretoria, South Africa.26-27. Wikipedia, Retrieved 29th April, 2023

Winnie L (2021), The death of a sacred tree led to the discovery of other wonders,digital image, BETH MOON, <https://www.atlasobscura.com/articles/africas-baobab-tree-photographs

Yakubu A., Gabriel A. & Folahan A (2017). Synthesis and Characterization of Cellulose Nanoparticles and Its Derivatives using a Combination of SpectroAnalytical Techniques. International Journal of Nanotechnology in Medicine & Engineering. ISSN 2474-8811: 66-67

Zahra, D., Abdan, K., Jawaid, M., Mohd, A. K, Mohammad, B., Masoud, D., Francisco, C., & Ishak, M. (2017). Mechanical and Thermal Properties of Natural Fibre Based Hybrid Composites: A Review. Pertanika Journal of Science & Technology. 25 (4): 1103 – 1122

Zorba, V., Stratakis, E., Barberoglou, M., Spanakis, E., Tzanetakis, P., Anastasiadis, S. H., & Fotakis, C. (2008). Biomimetic Artificial Surfaces Quantitatively

Reproduce the Water Repellency of a Lotus Leaf. Advanced Materials, 20(21), 4049-4054. https://doi.org/10.1002/adma.200800651

Zhu, K. & Schmauder, S. (2003). Prediction of the failure properties of short fibre reinforced composites with metal and polymer matrix. Composite Material Science. 28, pp. 743748

Zwawi, M. (2021). A Review on Natural Fiber Bio-Composites, Surface Modifications and Applications. Molecules , 26, 404. https://doi.org/10.3390/molecules26020404

APPENDICES

Methods for determining density/water absorption of Baobab fibre Effect of

Density and Water Absorption of urea formaldehyde resins

Table A1: Density properties of modified urea formaldehyde resins

Parameters	1	2	3	4	5
Volume (ml)	1.9	1.2	1.5	1.2	1.3
Initial Weight (g)	1.4561	1.085	1.2891	1.137	1.2718
Density (g/ml)	0.7281	0.9042	0.8594	0.9475	0.9783

Table A2: Water absorption properties of modified urea formaldehyde resins

Parameters	1	2	3	4	5
Volume (ml)	1.9	1.2	1.5	1.2	1.3
Initial Weight (g)	1.4561	1.085	1.2891	1.137	1.2718
Final weight (g/)	1.4582	1.0872	1.2913	1.1454	0.9783
Weight Difference (g)	0.0021	0.0023	0.0012	0.0084	0.0057
Water Absorption (%)	0.1442	0.212	0.1707	0.7387	0.4481

Graph tables for mechanical properties of modified UF

Table A3: Tensile Test Graph Table for Sample 1

Elastic Modulus	10.95MPa	Upper Yield	0.00MPa
Yield Strength	2.22MPa	Break Strength	0.11MPa
Break Elongation	141.36%	Elongation after fractyre	141.36%
Total Elongation	79.56%	Yield Elongation	2.16%
Yield Ratio	31.75%	Rp0.2	6.44MPa
Rp0.5	6.44MPa	Rt0.1	0.00MPa
Rt0.2	0.00MPa	Rt0.5	0.22MPa
Rp0.05	6.44MPa	MaxLoad	0.25kN
Max Elong	80.58mm	Lower Yield	0.00MPa
Tensile Strength	61.65MPa	Reduction of Area	100.00%
Non Proport Elongation	77.40%	Rp0.01	6.44MPa

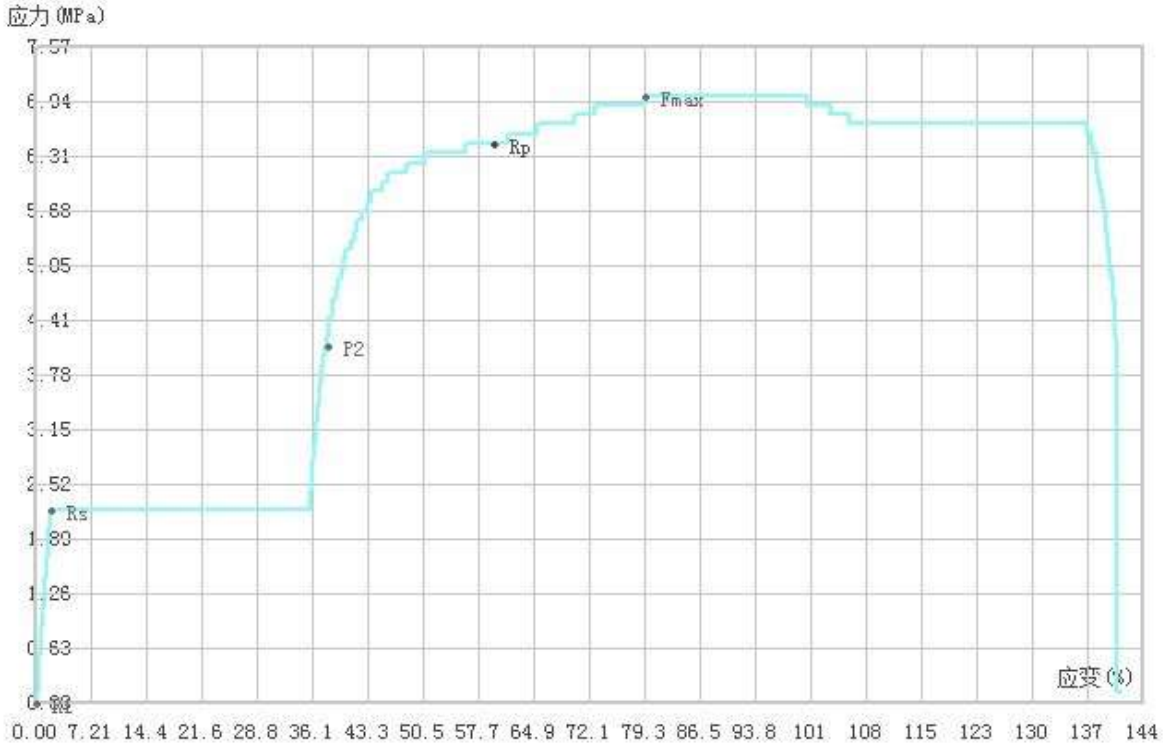

Figure A1: Tensile Test Graph Table for sample 1

Table A4: Tensile Test Graph Table for Sample 2

Elastic Modulus	80.18MPa	Upper Yield	0.00MPa
Yield Strenght	56.44MPa	Break Strength	71.33MPa
Break Elongation	75.39%	Elongation after fractyre	75.39%
Total Elongation	75.36%	Yield Elongation	72.54%
Yield Ratio	79.13%	Rp0.2	42.89MPa
Rp0.5	42.22MPa	Rt0.1	0.78MPa
Rt0.2	0.22MPa	Rt0.5	0.00MPa
Rp0.05	42.78MPa	MaxLoad	2.57kN
Max Elong	42.97mm	Lower Yield	0.00MPa
Tensile Strength	71.72MPa	Reduction of Area	100.00%
Non Proport Elongation	2.81%	Rp0.01	42.78MPa

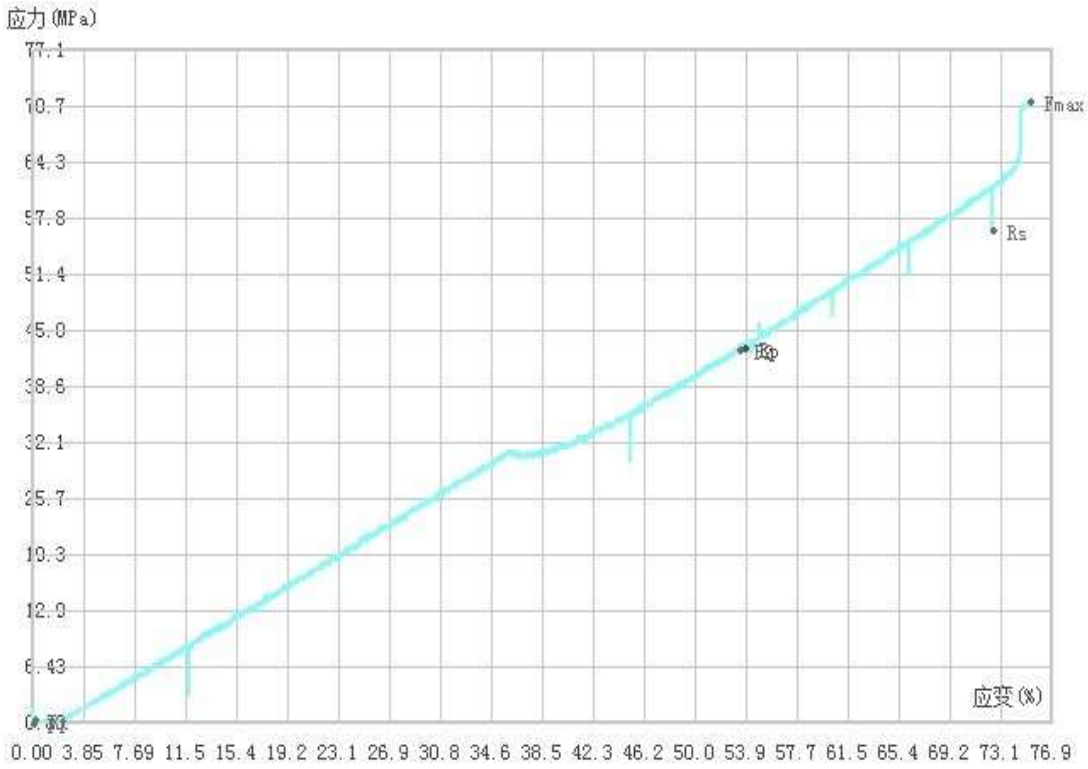

Figure A2: Tensile Test Graph Table for Sample 2

Table A5: Tensile Test Graph Table for Sample 3

Elastic Modulus	166.87MPa	Upper Yield	0.00MPa
Yield Strength	71.33MPa	Break Strength	95.11MPa
Break Elongation	66.19%	Elongation after fracture	66.19%
Total Elongation	65.18%	Yield Elongation	42.49%
Yield Ratio	71.41%	Rp0.2	71.89MPa
Rp0.5	73.11MPa	Rt0.1	3.67MPa
Rt0.2	3.67MPa	Rt0.5	4.22MPa
Rp0.05	69.44MPa	MaxLoad	3.60kN
Max Elong	37.73mm	Lower Yield	0.00MPa
Tensile Strength	79.72MPa	Reduction of Area	100.00%
Non Proport Elongation	22.69%	Rp0.01	68.11MPa

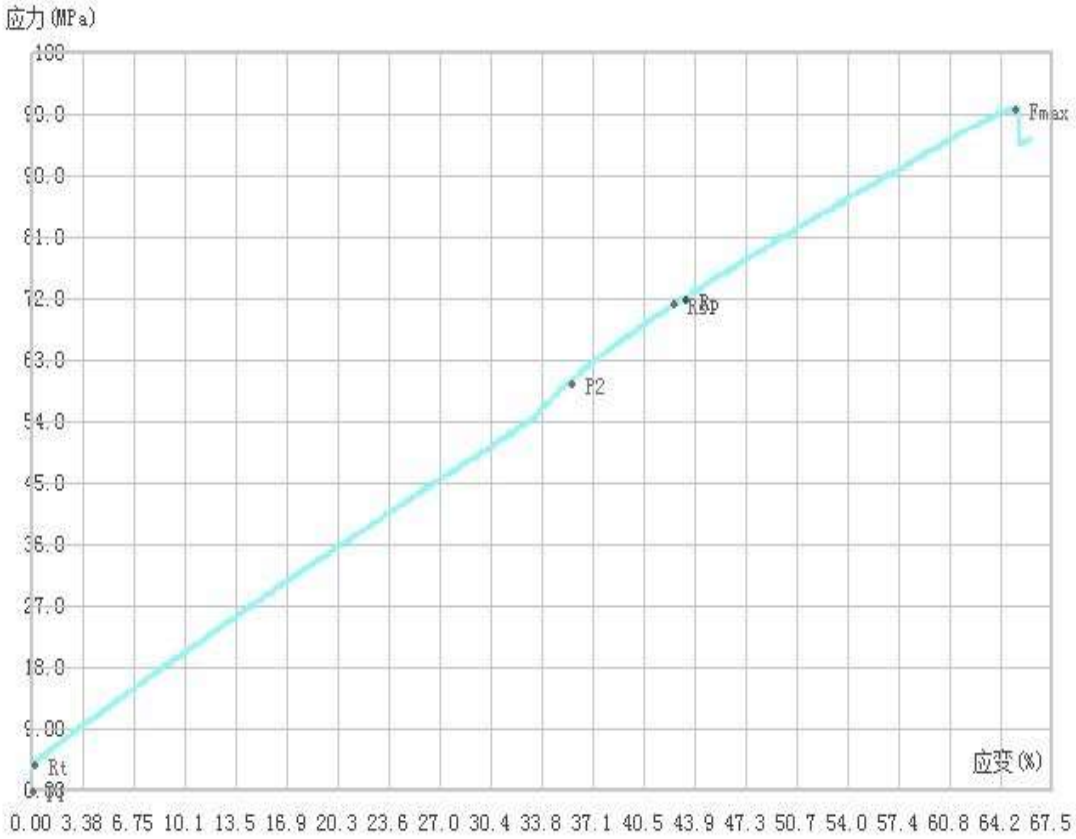

Figure A3: Tensile Test Graph for Sample 3

Table A6: Tensile Test Graph Table for Sample 4

Elastic Modulus	3.51MPa	Upper Yield	0.00MPa
Yield Strength	18.78MPa	Break Strength	18.11MPa
Break Elongation	1.#J%	Elongation after fractyre	1.#J%
Total Elongation	1.#J%	Yield Elongation	1.#J%
Yield Ratio	90.86%	Rp0.2	9.44MPa
Rp0.5	9.44MPa	Rt0.1	0.00MPa
Rt0.2	0.00MPa	Rt0.5	0.00MPa
Rp0.05	9.44MPa	MaxLoad	0.74kN
Max Elong	31.36mm	Lower Yield	0.00MPa
Tensile Strength	86.01MPa	Reduction of Area	100.00%
Non Proport Elongation	1.#J%	Rp0.01	9.44MPa

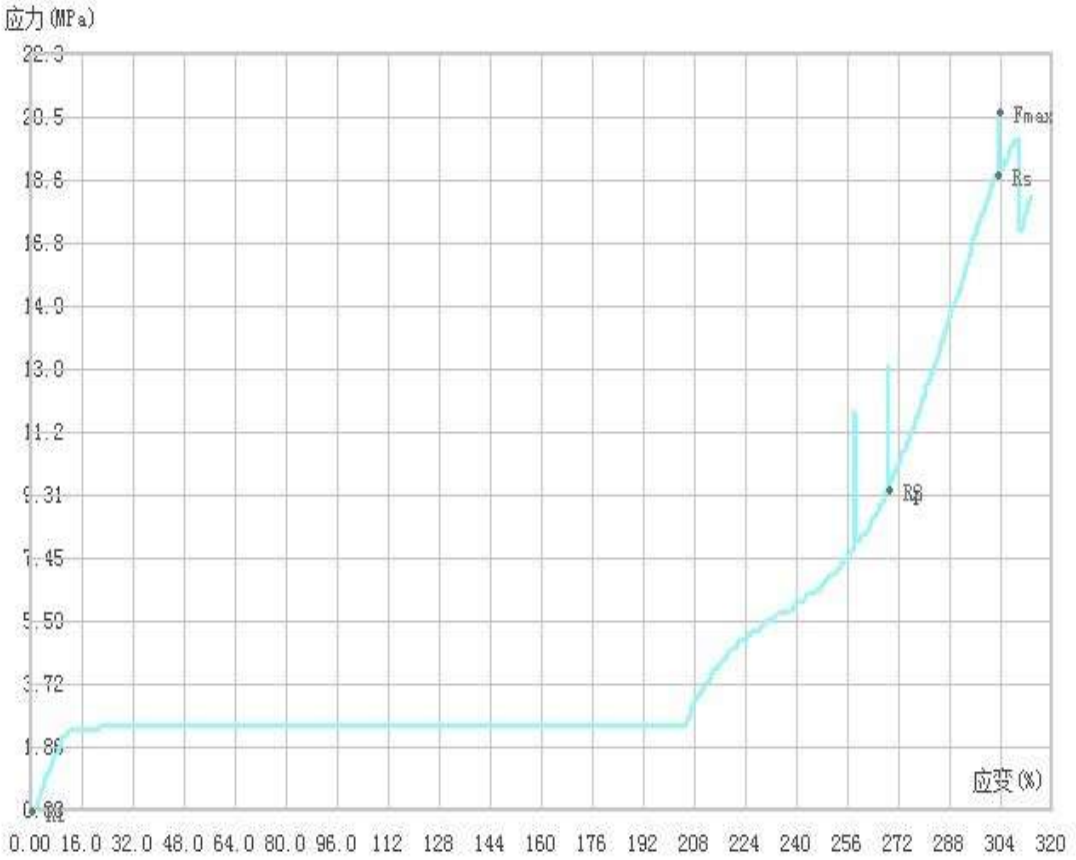

Figure A4: Tensile Test Graph for Sample 4

Table A7: Tensile Test Graph Table for Sample 5

Elastic Modulus	10.46MPa	Upper Yield	0.00MPa
Yield Strength	2.33MPa	Break Strength	0.67MPa
Break Elongation	63.25%	Elongation after fractyre	63.26%
Total Elongation	54.22%	Yield Elongation	1.62%
Yield Ratio	36.21%	Rp0.2	6.00MPa
Rp0.5	6.00MPa	Rt0.1	0.00MPa
Rt0.2	0.00MPa	Rt0.5	0.33MPa
Rp0.05	6.00MPa	Max Load	0.23kN
Max Elongation	35.42mm	Lower Yield	0.00MPa

Tensile Strength	84.72MPa	Reduction of Area	100.00%
Non Proport Elongation	52.60%	Rp0.01	6.11MPa

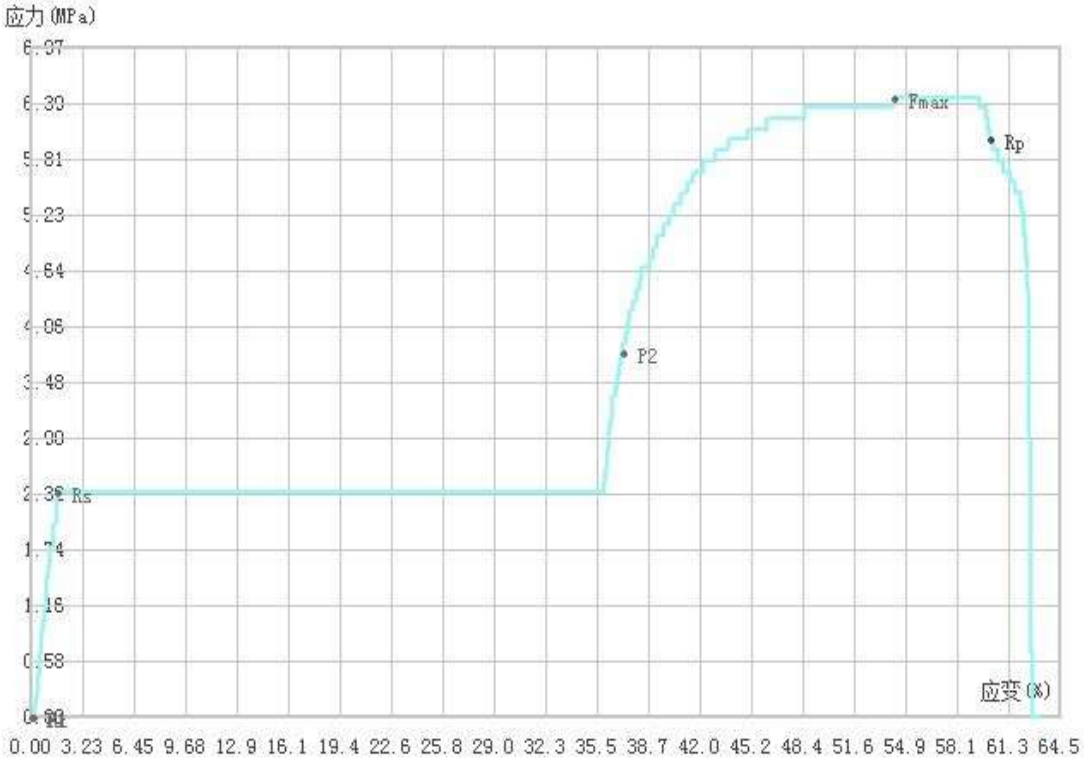

Figure A5: Tensile Test Graph for Sample 5